



The influence of ocean waves on Antarctic sea-ice albedo and seasonal melting, and physical-biological feedbacks

Robert A. Massom^{1,2,3}, Phillip A. Reid^{4,2}, Stephen G. Warren⁵, Bonnie Light⁶, Donald K. Perovich⁷, Luke G. Bennetts⁸, Petteri Uotila⁹, Siobhan P. O'Farrell¹⁰, Michael H. Meylan¹¹, Klaus M. Meiners^{1,2,3}, Pat Wongpan^{12,2}, Alexander D. Fraser^{12,2}, Alessandro Toffoli¹³, Giulio Passerotti¹⁴, Peter G. Strutton^{12,3}, Sean Chua^{1,2}, and Melissa Fedrigo¹

¹Australian Antarctic Division, Department of Climate Change, Energy, the Environment and Water, Kingston, Tasmania 7050, Australia

²Australian Antarctic Program Partnership, Institute for Marine and Antarctic Studies, Battery Point, Tasmania 7004, Australia

³ARC Australian Centre for Excellence in Antarctic Science, Institute for Marine and Antarctic Studies, Battery Point, Tasmania 7004, Australia

⁴Australian Bureau of Meteorology, Hobart, Tasmania 7000, Australia

⁵Department of Atmospheric and Climate Sciences, University of Washington, Seattle, Washington 98195, USA

⁶Polar Science Center and Department of Atmospheric and Climate Sciences, University of Washington, Seattle, Washington 98195, USA

⁷Thayer School of Engineering, Dartmouth College, Hanover, New Hampshire 03755, USA

⁸School of Mathematics and Statistics, University of Melbourne, Parkville, Victoria 3010, Australia. Formerly: School of Computer and Mathematical Sciences, University of Adelaide, Adelaide, South Australia 5005, Australia

⁹Institute for Atmospheric and Earth System Research/Physics, Faculty of Science, University of Helsinki, 00170 Helsinki, Finland

¹⁰CSIRO Environment, Aspendale, Victoria 3195, Australia

¹¹School of Information and Physical Sciences, University of Newcastle, Callaghan, New South Wales 2308, Australia

¹²Institute for Marine and Antarctic Studies, Battery Point, Tasmania 7004, Australia

¹³Department of Infrastructure Engineering, University of Melbourne, Parkville, Victoria 3010, Australia.

¹⁴School of Computing and Information Systems, University of Melbourne, Parkville, Victoria 3010, Australia

Correspondence to: Robert A. Massom (rob.massom@aad.gov.au)

Abstract. Identifying the processes that drive the rapid climatological retreat phase of Antarctica's annual sea-ice cycle is crucial to understanding, modelling and attributing observed trends and recent high variability in sea-ice extent, and to projecting future sea-ice conditions and impacts accurately. To date, the rapid annual retreat of Antarctic sea ice each spring–summer has been largely attributed to lateral and basal melting of ice floes, enhanced by wave-induced breakup of large floes. Here, based on observations and modelling, we propose that waves play important additional roles in generating previously-neglected surface and interior melting, by removing snow from small floes, flooding them, and pulverising them into slush. Results here show a resultant estimated reduction in albedo by 0.38–0.54, that increases melting by 0.9–5.2 cm day⁻¹ at 60–70°S compared to a snow-covered floe of first-year ice, and depending on surface type, wave-flooding coverage, latitude and ice density. Rapid proliferation of algae within and on the high-light and high-nutrient environment of the wave-modified ice reduces the albedo by a further 0.1 to increase the melt-rate enhancement to 1.1–6.1 cm day⁻¹. Melting is further accelerated



40 by a wave-induced ice–albedo feedback mechanism, similar to that associated with Arctic melt ponds but involving seawater rather than freshwater. This positive feedback is strengthened by ice–algal greening. Floe thinning and weakening by wave-melting initiate additional dynamic–thermodynamic feedbacks by increasing the likelihood of both wave-flooding and flexural breakup, leading to further floe melting. Wave melting and the associated physical–biological feedbacks will likely increase in importance in a predicted stormier and warmer Southern Ocean, and will also become more prevalent in a changing Arctic.

45 There are implications for global weather and climate, the health of the ocean and its ecosystems, fisheries, ice-shelf stability and sea-level rise, atmospheric and oceanic biogeochemistry, and human activities.

1 Introduction

1.1 Motivation and contribution

Each year from late austral spring through summer, the Southern Ocean encircling Antarctica undergoes a remarkable large-scale transformation with the areal retreat of its sea-ice zone (SIZ) from $\sim 18\text{--}20 \times 10^6 \text{ km}^2$ in September to $\sim 2\text{--}4 \times 10^6 \text{ km}^2$ in February. The retreat largely occurs over just a 3-month period (November through January), whereas the autumn–winter advance phase lasts for 7 months (Comiso et al., 2017a). By comparison, the annual cycle of Arctic sea ice is approximately symmetrical (i.e., 6 months advance and retreat), reflecting the different geographical setting and processes occurring there (Parkinson, 2014; Maksym, 2019). To date, the rapid annual retreat of Antarctic sea ice has been largely attributed to lateral and basal – rather than surface and interior – melting of its constituent ice floes (Eayrs et al., 2019a,b). The classical view is that this is driven by: (a) solar heating in leads (open-water gaps) between floes (Gordon, 1981) and within polynyas (Massom et al., 2003) that is related to the seasonal cycle (upturn) in incident solar radiation (Roach et al., 2022); and (b) upwelling of relatively warm deep waters in certain regions (Gordon, 1981). Moreover, melting in the Antarctic marginal ice zone (MIZ) has been identified as making the largest contribution to the mean annual ice retreat across the entire Southern Ocean (Kimura et al., 2022). The Antarctic MIZ is the tens- to hundreds of kilometres-wide region (Fraser et al., *subm.*) closest to the open ocean where the ice floes are regularly influenced by ocean surface waves (Wadhams, 1986; Bennetts et al., 2024), which break up larger floes and prevent smaller floes and pancakes from consolidating.

50

55

60

Here, and based on *in situ* observations, remote sensing and first-principle modelling calculations, we introduce additional and previously-unconsidered climatological factors that contribute to the rapid annual retreat of the Antarctic SIZ and which will likely increase in importance in a predicted stormier Southern Ocean (Young et al., 2020), as well as becoming more prevalent in a changing Arctic. These are the multiple roles of ocean waves in driving snow saturation and/or removal, creating seawater ponding and substantially decreasing the ice albedo, leading to surface and interior melting of small floes (while also contributing to basal and lateral melting) – both in the MIZ and the entire SIZ, i.e., adjacent to large open-water areas (leads and polynyas) and during deep swell-penetration events. Where present, snow inhibits/delays sea-ice melt (Eicken et al., 1995)

65

70 by virtue of its high albedo compared to bare sea ice (Perovich, 1996; Brandt et al., 2005; Zatko and Warren, 2015) and its



low thermal conductivity (Sturm and Massom, 2017). The snow cover strongly reflects incoming solar radiation and decreases its absorption by, and transmittance into and through, the underlying ice (Grenfell and Maykut, 1977; Grenfell and Perovich, 2004; Nicolaus et al., 2010). Moreover, snow buffers the ice below from air-temperature increases, including those associated with the frequent passage of storms, even in winter in the MIZ, e.g., Massom et al. (1997). Therefore, waves dramatically
75 alter the surface energy budget year round and the seasonal sea-ice melt rate, primarily by removing the snow cover to reduce the ice albedo and increase ice exposure to warm air temperatures, but also by overwashing floes with warm seawater.

We introduce the term *wave flooding* to encompass the processes of wave-induced seawater inundation, ponding and snow removal/modification. We also highlight a process that we call *wave pulverisation*, which is the breakdown of floes in the MIZ by their grinding together by incoming swells (see Massom et al., 2006). This process is distinct from flexural fracturing
80 (cf., Squire et al., 1995), and also contributes to a wider reduction in surface albedo and an increase in melt rate (compared to snow-covered floes). We introduce the term *wave melting* to refer to the combined contributions of wave flooding and pulverisation to the melting of the floe surface, the floe interior, and pulverised slush. We also propose that wave flooding and pulverisation processes lead to a proliferation of ice algae, which further decreases the ice albedo to enhance the surface and interior melting. Moreover, we propose that the wave-flooding processes invoke a positive ice-albedo feedback similar to
85 that associated with freshwater melt ponds (cf., Perovich et al., 2003; Perovich and Richter-Menge, 2009; Perovich et al., 2009) which form extensively on Arctic sea ice in summer (Fetterer and Untersteiner, 1998) from air temperature-driven snow melt and the pooling of the meltwater in surface depressions (Petrich et al., 2012) – albeit on different spatial and temporal scales but which also accelerate melting through spring–summer. We put forward that this *wave-driven ice-albedo feedback* is amplified by the algal greening (ice darkening), and that this further accelerates melting in concert with two other wave-driven
90 positive feedback mechanisms. These are a *wave flooding-ice melting feedback* and a *wave flooding-floe fragmentation feedback*.

1.2 Context

To date, and in contrast to the Arctic (e.g., Tsamados et al., 2015), floe-surface melting and interior melting and their associated ice-albedo feedbacks have remained largely neglected as climatological factors contributing to the rapid annual retreat of the
95 Antarctic SIZ. This neglect is based on the dual premise that Antarctic sea ice largely retains its high-albedo and insulative snow cover into summer (Massom et al., 2001; Eayrs et al., 2019) while also lacking Arctic-like freshwater melt ponds (Andreas and Ackley, 1982; Drinkwater and Liu, 2000), apart from a few isolated observations (e.g. Takahashi, 1960; Corkill et al., 2023). The general lack of surface melt ponds on Antarctic sea ice has been attributed to the radiative and turbulent surface heat fluxes occurring there (Vihma et al., 2009). Complete synoptic-scale snow-melt episodes do occur at lower
100 latitudes due to extreme temperature increases and even rainfall associated with the passage of storms, including in winter in the MIZ, but those events tend to be somewhat localised and short-lived/ephemeral (Massom et al., 1997).



Given these factors, the generally-used conceptual model for the broad climatological annual retreat of Antarctic sea ice is that each late-spring and summer, wind-driven Ekman divergence (Gordon and Taylor, 1975) associated with a twice-yearly deepening and poleward contraction of the circumpolar trough of sea-level pressure known as the Semi-Annual Oscillation (van Loon, 1967; Eayrs et al., 2019) pushes ice floes northwards into warmer waters where they melt. In addition, the ice divergence creates dark (low-albedo) leads between floes that strongly absorb incoming solar radiation (Gordon, 1981; Enomoto and Ohmura, 1990). With the seasonal upturn in insolation following the September equinox (Roach et al., 2022), solar heating of the ocean's mixed layer then drives both lateral and basal melting of the floes (Maykut and Perovich, 1987). This further activates a positive "ocean–ice albedo feedback" (Nihashi and Cavalieri, 2006) related to the difference in albedo between sea ice and open water, whereby solar heating in leads enhances lateral melt of floes and increases the open-water area (decreases the ice concentration), to further enhance ice melt and so on (Ebert and Curry, 1993; Curry et al., 1995; Ohshima and Nihashi, 2005; Kashiwase et al., 2017).

Currently, ocean waves are largely considered to influence sea-ice melting only in terms of their important role in fracturing the MIZ ice cover into smaller floes (cf., Wadhams, 1986; Squire, 2007; Kohout et al., 2016). Small floes are more mobile and have a larger perimeter per unit area (Maykut and Perovich, 1987; Toyota et al., 2006) compared to larger floes, leading to relatively larger rates of lateral melting (Steele, 1992; Asplin et al., 2012; 2014; Perovich and Jones, 2014; Kohout et al., 2014) and basal melting (Horvat and Tziperman, 2018). Sea-ice models now include the influence of waves on floe-size distributions (e.g., Bennetts et al., 2017; Roach et al., 2019; Bateson et al., 2020) – but not the role of waves in driving coupled dynamic-thermodynamic processes involving year-round flooding, snow removal, pulverisation and albedo reduction that lead to seasonal surface and interior melting of small wave-fragmented floes and wave-pulverised slush, as proposed here.

1.3 Significance

There is strong motivation to identify, understand and model the complex atmosphere–ice–ocean interaction processes and feedback mechanisms responsible for driving the mean rapid retreat phase of Antarctica's annual sea-ice cycle, including the role of the MIZ (Saiki et al., 2021). Such knowledge is crucial to addressing the inability of contemporary models to reproduce the rate and magnitude of the mean annual sea-ice retreat phase observed in the satellite record accurately (cf., Eayrs et al., 2019; Roach et al., 2020), towards attributing observed Antarctic sea-ice trends and variability and providing more-confident future projections (e.g., Notz and Bitz, 2017; Maksym, 2019; NAS, 2017; Roach et al., 2020). This priority need is underpinned by mounting concern over recent Antarctic sea-ice loss and its serious implications for Antarctica and the Earth system (Kennicutt et al., 2014; Massom et al., 2018; Meredith et al., 2019). Since 2012, Antarctic sea-ice coverage has unexpectedly switched to a state of high variability (Turner and Comiso, 2017; Hobbs et al., 2024), with record high sea-ice extents in 2012–2014 (Reid and Massom, 2015) plummeting to record lows since 2016 – and with the biggest deficit occurring not only in the spring–summer melt period (Parkinson, 2019) but also in autumn–winter in 2023 (Reid et al., 2024) and 2024 (Reid et al., in press).



The unanticipated rapidity and magnitude of this apparent regime change raises concerns around potential acceleration of future Antarctic sea-ice loss in response to resultant changes in albedo and the surface energy budget (Riihelä et al., 2021) and activation and amplification of sea ice-related albedo feedback mechanisms (Goosse et al., 2018). At the same time, a change in the albedo of the Antarctic SIZ has the potential to amplify high-latitude climate warming in the Southern Hemisphere, as it has in the Arctic (Manabe and Stouffer 1980; Meehl and Washington, 1990; Holland and Bitz, 2003; Screen and Simmonds, 2010). Model analyses by Goosse et al. (2023) highlight the key role of albedo in the annual Antarctic sea-ice cycle and as a prime target for process understanding and model development. Here, we provide mechanisms (wave flooding, pulverisation and greening) for determining and modifying the surface albedo, as well as the thickness distributions and volume of the sea ice and its snow cover – all of which are major unknowns in the global climate system and severely compromise modelling and predictive capability (Maksym et al., 2012; Webster et al., 2018).

While this study is limited in terms of coordinated large-scale observations of wave flooding and melting across the Antarctic MIZ and SIZ, the synthesis of available observations given here is timely and presents a new paradigm in our understanding of factors controlling the seasonal retreat/melt phase of Antarctic sea ice. Our aim is fourfold:

- (1) to stimulate targeted cross-disciplinary observations of the wave-related surface melt processes and feedbacks we describe, towards quantification of current unknowns relating to their distribution and characteristics in space and time;
- (2) to encourage further testing of the new hypotheses presented here, not only in the Antarctic but also in the Arctic;
- (3) to encourage investigation of the contribution of wave flooding and wave melting to primary production and key biogeochemical processes in the SIZ, and to the ocean biological carbon pump and the uptake of atmospheric CO₂ by the ocean; and
- (4) to encourage incorporation and analysis of wave flooding and resultant wave melting processes and feedbacks in climate and Earth system models and sensitivity studies, in order to help address the critical key deficiencies in model prediction outlined above.

Given the current lack of requisite data, this study does not attempt a detailed quantitative evaluation of the characteristics and effects of wave flooding and wave pulverisation and the spatio-temporal coverage and overall magnitude of wave melting and its contribution to the annual sea-ice cycle. The primary contribution of this work is on making a first estimate of the effect of wave flooding and wave pulverisation on the daily melt rate of an idealised ice floe (and/or area of wave-pulverised slush) in the Antarctic SIZ in summer by changing the ice albedo (α) in the surface radiation energy budget. The overall aim is to show that the effect could be significant, and is therefore worthy of further investigation by targeted fieldwork and modelling.

2 Data and techniques

2.1 Observations

Wave melting phenomena and processes are identified based on shipborne observations and photographs acquired from multiple voyages across the Antarctic SIZ, particularly the MIZ, and from the literature (e.g., Ackley, 1985; Massom, 1991;



Ackley and Sullivan, 1994; Massom et al., 1997, 1998, 1999, 2001, 2006). As no direct measurements are available for albedos of wave-flooded and wave-pulverised ice, we use proxy estimates of albedos of the different surface types derived from measurements made from ships and helicopters, as described in Sect. 3.2 below. Daily sea-ice concentration for calculating the distance to the ice edge (Sect. 3.1.2) is based on satellite passive-microwave ice concentration data dating back to 1979 (Cavalieri et al. 1996, updated yearly). The sea-ice edge is delineated by the 15% ice-concentration isoline.

2.2 Computing radiative transfer and melt-rate enhancement

Here, we consider the effect of wave flooding and wave pulverisation only on the shortwave rather than longwave properties of an ice floe/area of wave slush, which is to reduce the sea-ice albedo. The longwave (infrared) emissivities of snow, ice and water are all close to 100% (Warren, 1982, 2019), so the only longwave effect of wave flooding is to increase the longwave emission slightly by increasing the surface temperature of the ice floe, bringing it up to $\sim 0^\circ\text{C}$. Our computation starts with the daily-average incident solar flux at the top of the atmosphere, F_{TOA} (in W/m^2), and then multiplies it by the atmospheric transmittance over Antarctic sea ice, τ_a , to obtain the solar flux at the surface (F_{sfc} , in W/m^2), as

$$F_{sfc} = \tau_a F_{TOA}. \quad (1)$$

Following Fitzpatrick and Warren (2005; FW05), and as τ_a is not directly available, we take two steps to obtain F_{sfc} . We first obtain the transmittance, τ_{clr} , for clear sky (shown in Fig. 7 of FW05 as a linear fit versus solar zenith angle θ , such that

$$\tau_{clr} = 1.03 - 0.0046 \theta, \quad (2)$$

with θ in degrees. Then we apply the “cloud radiative forcing” CRF as a correction, to obtain F_{sfc} as

$$F_{sfc} = \tau_{clr} F_{TOA} + CRF_d, \quad (3)$$

where CRF_d is the downward shortwave cloud radiative forcing in W/m^2 (measured by FW05 and plotted in their Fig. 10), which is a negative quantity, indicating that clouds reduce the downward solar flux at the surface.

We estimate the albedo change (decrease), $\Delta\alpha$, caused by wave flooding of a snow-covered floe of wave pulverisation to be

$$\Delta\alpha = \alpha_s - \alpha_w, \quad (4)$$

where α_s is the albedo of a snow-covered floe of first-year ice (FYI) (e.g., floe marked D in Fig. 1c), and α_w is the albedo of a wave-overwashed floe (e.g., floes marked A and B in Fig. 1a), a wave-ponded floe (e.g., labelled C and E in Fig. 1c) or wave-pulverised slush (e.g., Fig. 1i). Multiplying F_{sfc} by $\Delta\alpha$ gives the wave-washing radiative forcing, RF_w , of wave-flooded or wave-pulverised as

$$RF_w = \Delta\alpha F_{sfc}, \quad (5)$$

which is in units of W m^{-2} . Equation (5) holds for a single idealised sea-ice slab, or an idealised small area of (unconsolidated) wave-pulverised slush.



195 To obtain regional averages of radiative forcing, $RF_{w,avg}$, we would multiply RF_w by the ice concentration, C , and the fraction of floe area affected by wave flooding, f_w , to give:

$$RF_{w,avg} = C f_w RF_w = C f_w \Delta \alpha F_{sfc}. \quad (6)$$

This calculation could be refined by using the frequency-distributions of (a) ice concentration, (b) solar zenith angles, (c) cloud thicknesses, and (d) the fractional coverages of the different wave-washing types, to get $RF_{w,avg}$ as a function of latitude, longitude and month, i.e., similar to Eq. (8) of Fitzpatrick and Warren (2007). However, that refinement is also beyond the scope of this study, the aim of which is simply to show that wave flooding and wave pulverisation could enhance sea-ice melting, arguing that it is worthy of further investigation.

To estimate the change in melt rate of sea ice due to the radiative forcing, we divide the radiative forcing (Eq. 5) by the sea-ice density, $\rho = 905 \text{ kg m}^{-3}$ (Fang et al 2022), and the latent heat of fusion, $L = 334 \text{ J g}^{-1}$ (Fang et al 2022), to obtain

$$205 \quad dh/dt = RF_w / (\rho L), \quad (7)$$

where h is the sea-ice thickness and t is time.

3 Results

3.1 Wave flooding and wave melting processes

Based on available observations, we identify six coupled dynamic–thermodynamic (and biological) processes driven by waves that operate year round and increase surface and interior melting of small floes (typically <5 m diameter) that are the product of wave breakup of larger floes. Five of these processes, *wave overwashing*, *wave buffeting* and associated *wave ponding*, *wave deformation ponding* and *wave compression flooding*, involve partial or complete snow removal and/or snow wetting and inundation of the ice surface with seawater, plus (in the case of wave ponding) seawater pooling on the ice. Further, we propose *wave pulverisation* as a sixth wave-induced process that contributes to Antarctic seasonal sea-ice melting by mechanically grinding down small floes and fragments of brash ice into a combined slurry of ice and snow slush, which melts more rapidly. We term this *wave slush*. An additional (seventh) process – *wave greening* – involves darkening of the ice due to increased algal growth in surface wave ponds, the interior of the snow-free ice, and wave-pulverised slush, in turn increasing light absorption and ice melt (cf., Zeebe et al., 1991). Example images are shown in Fig. 1, with schematic representation of wave-fracturing, wave-flooding and wave-pulverisation processes in Fig. 2. The images are all from the East Antarctic sector in late austral winter to early spring, apart from the wave-pulverisation and slush images (Fig. 1i, j) which are from the Bellingshausen Sea. All are oblique views from the ship (the RSV *Aurora Australis*), apart from Fig. 1g which is a vertical aerial image.

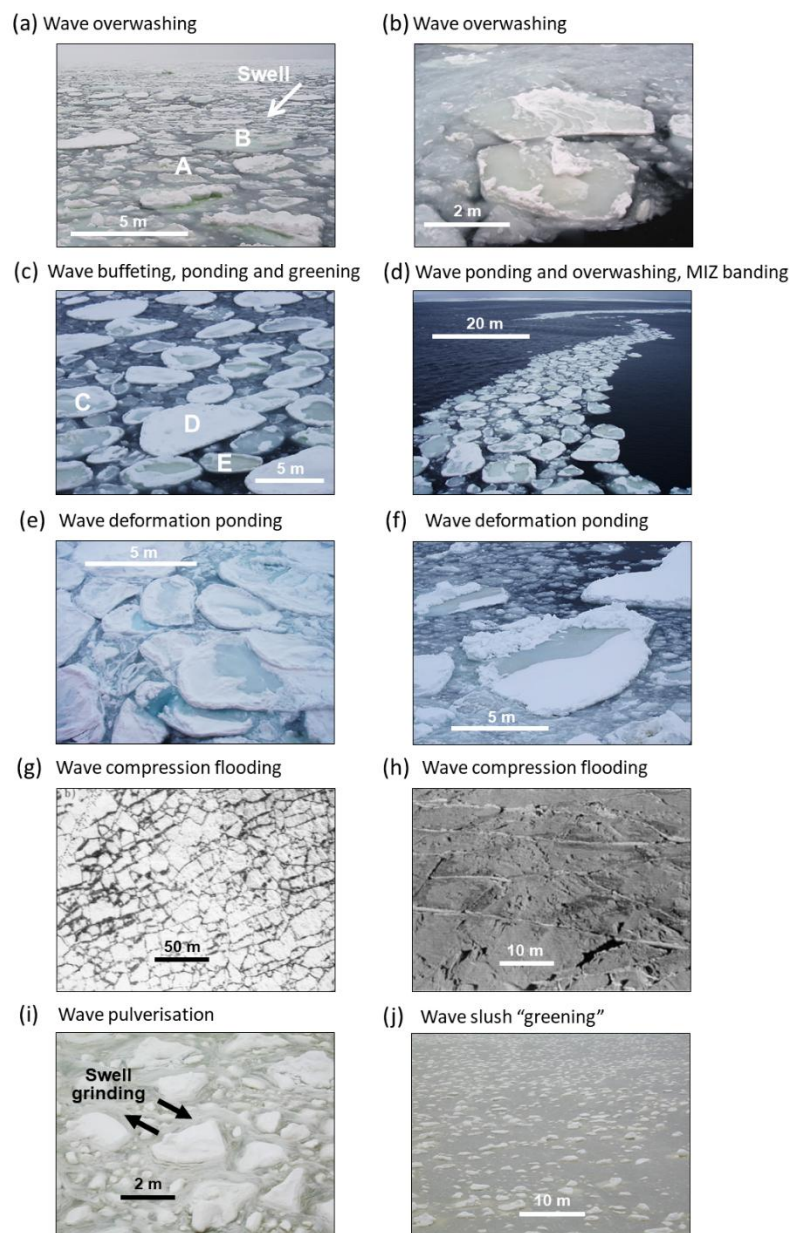


Figure 1: Photographic examples of wave flooding and wave pulverisation processes, with estimates of ice thickness (h_i) and surface water depth (h_w): a-b) wave overwashing ($h_i \sim 100$ cm, $h_w \sim 1-5$ cm); c) wave buffeting, wave ponding and wave greening ($h_i \sim 70$ cm, $h_w \sim 5$ cm); d) marginal ice zone banding with wave ponding and wave overwashing ($h_i \sim 50-70$ cm, $h_w \sim 5$ cm); e-f) wave deformation ponding ($h_i \sim 70-100$ m, $h_w \sim 5-20$ cm); g-h) wave compression flooding from aerial photography and from the surface ($h_i \sim 70$ m); i) wave pulverisation (wave-slush thickness $\sim 0.50-1.00$ m), with black arrows denoting wave churning; and j) wave-slush greening (wave-slush thickness $\sim 0.5-1.0$ m).



230

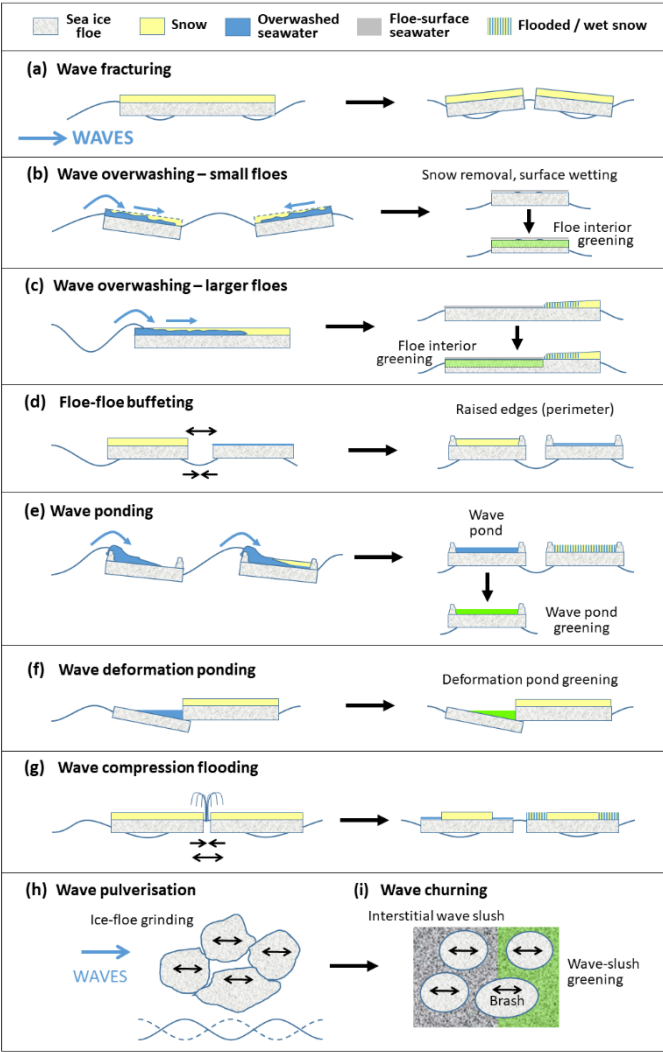


Figure 2: Schematic representation of a) wave fracturing; b-c) wave overwashing; d) wave buffeting; e) wave ponding; f) wave-deformation ponding; g) wave-compression flooding; h) wave pulverisation; and i) wave churning. Representative images b-i are shown in Fig. 1.

235 Wave-flooding processes are not to be confused with flooding due to floe-surface submergence under the weight of overlying snow (Wadhams et al., 1987; Massom et al., 2001). This latter style of flooding is widespread across the Antarctic SIZ (Eicken et al., 1994; Maksym and Markus, 2008), but it seldom results in complete snow removal and exposed ponding because only the lowest part of the snowpack is flooded.

3.1.1 Wave overwashing



240 Wave overwashing is a widespread phenomenon and process in the outer Antarctic MIZ (Massom et al., 1997; 1998), as well as the outer Arctic MIZ (Massom, 1991). Floes smaller than or comparable to the prevailing wavelengths move with the incoming waves but slightly out-of-phase with them, such that overwashing is generated at the leading and trailing floe edges as they pitch below the ocean surface (Skene et al., 2015; Toffoli et al., 2015; Dolatshah et al., 2018; Nelli et al., 2020). This causes seawater to flow (wash) back and forth across their surfaces (Fig. 1a,b; Fig. 2b), where it can either push the snow cover
245 into the water and/or turn it into a slush layer on the floe surface. In contrast, floes larger than the prevailing wavelengths, and directly exposed to open water, are overwashed by waves breaking over their leading edge and onto the floe surface (Passerotti et al., 2022; Fig. 2c). Wave overwashing also thrusts sea-ice blocks onto the surfaces (margins) of small floes, to decrease the local floe freeboard and increase the likelihood of further overwashing and flooding (see Sect. 3.1.3 below).

Wave overwashing is not restricted to the MIZ, as it also affects floes adjacent to large leads and polynyas, as observed in the
250 Weddell Sea (Massom et al., 1997) and the East Antarctic sector (Massom et al., 1998). This is due to the prevalence of wind waves there, generated by katabatic winds in coastal regions, e.g., within polynyas (cf., Ackley et al., 2022; Herman and Bradtke, 2024) and the frequent passage of storms across the wider SIZ (cf., Godfred-Spenning and Simmonds, 1996; Uotila et al., 2011). For example, Ackley et al. (2022) observed significant wave heights exceeding 2m in the Terra Nova Bay Polynya (Ross Sea) in May. Large leads are a prevalent feature within the Antarctic SIZ (Dubey et al., 2025) due to its largely-
255 divergent nature (Worby et al., 1998), with lead widths of up to 6500 m observed in the Weddell Sea by Muchow et al. (2020), and there is also widespread distribution of recurrent and persistent coastal and open-ocean polynyas (Barber and Massom, 2007).

3.1.2 Wave buffeting and wave ponding

Wave buffeting is the constant collision, jostling and rotation of small floes driven by incoming waves, which rounds off their
260 angular edges and creates decimetre-scale raised rims (Fig. 1c; Fig. 2d). Where these rims form around the entire floe perimeter, they act as mini-ice levées that entrap and retain seawater introduced onto the surface by wave overwashing (Fig. 2e), and/or via the upward movement of seawater through the ice if it is permeable and has a negative freeboard. We term these saline ponds *wave ponds*. Although wave ponds in some ways resemble seasonal Arctic melt ponds, they are saline rather than freshwater (low salinity) and occur year-round, i.e., they are not confined to the summer melt season and form
265 faster than Arctic melt ponds (cf., Lüthje et al., 2006; Webster et al., 2022). Wave-pond formation is also likely influenced by the effect of the additional mass of rim ice and rafted ice blocks in modifying the floe isostasy and decreasing the floe freeboard. Wave ponds can be maintained by constant wave overwashing, but they can also freeze and accumulate a snow cover in the cold season and where wave energy dies down.

In the typical example shown in Fig. 1c, the scene is visually estimated to comprise approximately 10% open water and 25%
270 combined brash ice and wave slush ice by area, with flooding/ponding covering about one third of the remaining coverage of



small ice floes. This example, from 11 October 2007 at $\sim 62.5^\circ$ S and 123.7° E, is about 25 km south of the ice edge as demarcated by the 15% sea-ice concentration isoline.

3.1.3 Wave deformation ponding

Surface ponding also occurs where incoming waves drive the interaction and deformation of small floes, leading to the
275 localised replacement of snow cover with saline water in pools up to a few metres across (Fig. 1e,f; Fig. 2f). In this case, waves force rafting of floes and the mechanical pile-up of ice rubble and/or pressure ridging (Dai et al., 2004; Bennetts and Williams, 2015; Sutherland and Dumont, 2018), which can depress part of the floe surface below sea level leading to seawater ponding when there is connection to the underlying ocean (Massom et al., 1997, 1998). We term this *wave-deformation ponding*. Wave-deformation ponds have been observed to cover ~ 5 –10% of the total surface area of the sea-ice floes about
280 200 km poleward of the ice edge in winter, in both the northwestern Weddell Sea (Massom et al., 1997) and the western Pacific Ocean sector (Massom et al., 1998).

In addition, wave-induced fracturing of larger floes near an existing pressure ridge can place the adjacent ice surface out of isostatic balance due to the weight of the ridge, leading to submergence, flooding and ponding of the resultant smaller floe as it readjusts (Ackley and Sullivan, 1994). In the Weddell Sea, such ponding can be prevalent in the outer 200 km of the SIZ,
285 and in the highly-deformed ice in the western outflow region of the Weddell Gyre, i.e., 40 – 60° W (Ackley and Sullivan, 1994). Flooded areas caused by pressure-ridge loading have been termed *surface-saline ponds* by Ackley and Sullivan (1994). Similar ponds also occur even deeper into the SIZ, due to deformational processes not related to waves, e.g., convergence in the ice field causing surface depression and ice cracking adjacent to pressure ridges (Ackley, 1985; Massom et al., 1997).

3.1.4 Wave compression flooding

Under certain circumstances, long-period swells penetrate more deeply into the Antarctic SIZ, i.e., hundreds of kms in from the ice edge (Liu and Mollo-Christensen, 1988; Nose et al., 2023; cf., Morris et al., 1998; Worby et al., 1998; Kohout et al., 2014). In addition to driving wave-deformation ponding, deep swell penetration can lead to *wave compression flooding* in extensive areas of undeformed FYI (Massom et al., 1999). By this process (Fig. 2g) and in the example given in Fig. 1g-h from the East Antarctic SIZ in August 1995, incoming swells caused linear lateral and transverse through-cutting breaks
295 (cracks) in large floes of uniform thickness. These cracks opened and then closed a few seconds later with the passage of each wave crest and trough, leading to compression of seawater between the two converging ice plates (Massom et al., 1999). This resulted in the "squirting" of seawater onto the surface of the newly-created, small angular floes around their perimeter (Worby et al., 1998). Analysis of aerial photographs along the $139^\circ 15'$ E meridian revealed that this wave-compression flooding event affected a zonal band ~ 70 km wide and up to 360 km south of the ice edge (Massom et al., 1999). This process wetted and
300 darkened an estimated 20% of the surface of 100%-concentration sea ice (seen as a greying of the snow cover adjacent to the cracks, determined from the aerial photos). While the frequency of wave-compression events is unknown, they may occasionally cause flooding of floes deep in the SIZ, irrespective of season.



3.1.5 Wave pulverisation

While there has been emphasis on the role of waves in the flexural breakup of larger floes into smaller floes in the MIZ (e.g., Kohout et al., 2014), we highlight an additional widespread, yet largely neglected, wave-driven process in floe breakdown and melting. This is the lateral grinding together of small floes by incoming swells (Fig. 2h), resulting in the mechanical pulverisation of the floes and their snow cover into an unconsolidated mix of wave slush and brash fragments (Massom et al., 2006). In the colder months, this wave slush is supplemented by frazil ice formation.

In an October 2001 observation from the Bellingshausen Sea (Fig. 1i), persistent north-westerly winds compacted the MIZ against the Antarctic Peninsula, while a 2–3 m swell mechanically ground down the ice cover over tens of kilometres in from a linear ice edge (Massom et al., 2006). This created a continuous (100% cover) but unconsolidated agglomeration of brash ice fragments (<~1 m across) separated by an interstitial slurry of slush ice that was constantly churned and reworked by the incoming swells. Interstitial slush ice and brash ice also occur between larger contiguous floes in wave-affected areas, as in the examples of wave overwashing and ponding given in Fig. 1a-b and Fig. 1c-d, respectively.

3.1.6 Wave greening

We propose that wave flooding and associated snow removal also drive the rapid proliferation of ice algae within wave ponds (see floe E in Fig. 1c) and/or in the ice column (particularly in late spring–summer) – and that this *wave greening* (darkening due to high chlorophyll and other pigment content) intensifies the sea-ice melt-rate enhancement by further reducing the ice albedo (see Sects. 3.2 and 3.3). Light attenuation by snow is a major limiter of ice-algal growth (Arrigo et al., 2014), and snow-cover removal by waves increases the exposure of low-light-adapted algae to substantially higher amounts of photosynthetically-active radiation. Wave flooding likely also introduces biogenic material and nutrients onto floe surfaces, where they are retained in wave ponds and/or continually replenished by wave flooding. While no direct measurements of wave-pond habitats (“floe oases”) are yet available, observations of saline deformation ponds show that they can support high algal biomass (chlorophyll content) (Kottmeier and Sullivan, 1990; Ackley and Sullivan, 1994; Garrison et al., 2003; Arrigo et al., 2014). This greening of wave (and deformation) ponds contrasts with Arctic freshwater meltponds, which generally contain low algal biomass due to low nutrient concentrations (Arrigo et al., 2014).

In the case of the wave pulverisation depicted in Fig. 1i and Fig. 2i, the mechanical grinding and churning of the ice and resultant release of ice algae contained within it created an unconsolidated agglomeration of green slush/frazil-ice slurry interspersed with brash-ice fragments <1 m across. This exposed the ice algae to significantly higher light and nutrient levels than in a snow-covered floe, leading to an intense “intra-ice algal bloom” in October, i.e., unusually early in the sunlit season and relatively far south at ~65°S (Massom et al., 2006).



3.2 Wave modification of sea-ice albedo

335 Spectral albedo has been measured from ships and helicopters for multiple types of Antarctic sea ice, both bare and snow-covered. Brandt et al. (2005) and Zatko and Warren (2015) summarise the measured albedo values, where spectral values are integrated over wavelength (weighted by the solar spectral flux) to obtain band-average albedos for narrow- and broad-bands, and for both clear and cloudy skies. Here we use averages over the entire solar spectrum (290–3000 nm wavelengths), which we call “broadband albedo” (Table 1a). We list the albedos for cloudy sky rather than clear sky, as they are the most relevant

340 to the Antarctic SIZ, given that average cloud coverage there exceeds 80% in spring–summer (Warren et al., 1988; Fitzpatrick and Warren, 2007). Immediately apparent is the strong sensitivity of sea-ice albedo to even a thin layer of snow. Snow-free FYI floes that are <0.7m and >0.7 m thick have average broadband albedos which are 0.3 less than their snow-covered counterparts, respectively. Therefore, snow removal is of crucial importance in terms of its effect on the radiation energy budget and the seasonal melt rate of sea ice.

345 a.

<i>Surface type</i>	<i>Albedo range</i>	<i>Average albedo</i>
Open water	0.06-0.07	0.07
First-year ice (<0.7 m), bare	0.41-0.49	0.45
First-year ice (<0.7 m) with 2-4 cm snow	0.70-0.78	0.74
First-year ice (>0.7 m), bare	0.50-0.58	0.54
First-year ice (>0.7 m) with >3 cm snow	0.82-0.87	0.84
Wave-pulverised ice plus pancake ice, one case only (Allison et al., 1993 Figure 12)	0.68	
Snow-slush (average and range of 4 cases)	0.35-0.59	0.46

b.

<i>Wave-affected surface type</i>	<i>Photos in Figure 1</i>	<i>Albedo range</i>	<i>Average albedo</i>	<i>Aa</i>
Overwashed first-year ice	a, b	0.35-0.59	0.46	0.38
Wave-compression flooded	g, h			
Wave-pulverised slush	i			
Wave-pulverised slush – green	j	0.25-0.49	0.36	0.48
Wave pond	c, d	0.2-0.4	0.3	0.54
Wave deformation pond	e, f			
Wave pond, bare ice* – green	c	0.1-0.3	0.2	0.64

Table 1. Broadband albedos for surface types in the Antarctic SSIZ, under a cloudy sky: (a) measured for open water, bare ice, snow-covered ice, and slush (Brandt et al., 2005; Zatko and Warren, 2015); and (b) estimated for wave-

350



flooded and wave-pulverised sea-ice types, and albedo difference/reduction ($\Delta\alpha$) compared to first-year ice >0.7 m thick with a >3 cm snow cover. *Bare ice refers to wave-overwashed ice with no snow cover.

Albedo has not been measured for wave-flooded or wave-pulverised ice floes, excepting Allison et al. (1993) who reported an albedo of 0.68 for a mixture of pancake ice, nilas and brash ice. However, that albedo value depends on the relative amounts of the three ice types present, so we do not use it in our calculations. Instead, we use Zatko and Warren (2015)'s measured albedo for four cases of slush formed by snow blowing into a lead in the Antarctic SIZ, as a surrogate for slush ice formed by wave pulverisation processes (Fig. 1i), wave compression-flooded ice (Fig. 1g,h), and wave-overwashed FYI (Fig. 1a,b).

To represent wave ponds (Fig. 1c,d) and wave deformation ponds (Fig. 1e,f), we use albedos measured on Arctic melt ponds with similar appearance (Light et al., 2022). Most Arctic melt-ponds are darker than Antarctic wave ponds, because melt ponds overlay waterlogged ice (the snow is long-gone) whereas wave ponds are typically brighter as they consist of slush or water over bright ice. However, many Arctic melt ponds do resemble the wave ponds shown in Fig. 1c-f, and those melt ponds are the ones we use as surrogates. The surrogate broadband albedo values for the different wave-affected surface types are given in Table 1b. Table 1b also includes albedo estimates for wave-ponded, bare and wave-pulverised ice types modified by wave greening. In the absence of direct measurements and for the purpose of this study, the greening is estimated (assumed) to reduce the albedos of these types by an additional 0.1 compared to their “non-green” counterparts.

We compare these surrogate average broadband albedo values with that observed for FYI with thickness >0.7 m and a snow layer >3 cm thick ($\alpha = 0.84$) to determine the change (decrease) in average broadband albedo ($\Delta\alpha$) for the four different wave-affected surface-type categories. Values of $\Delta\alpha$ are: 0.38 for overwashed FYI, wave-compression flooded ice, and wave-pulverised slush; 0.48 for wave-pulverised slush (green); 0.54 for wave ponds and wave deformation ponds; and 0.64 for wave pond or bare ice that are greened. As outlined in Sect. 2.2 (Eqs. 4-6) these values of $\Delta\alpha$ then form the basis for a first crude estimate of the resultant increases in the melt rates of the wave-affected ice types in the Antarctic SIZ in summer due to wave flooding and wave pulverisation, and compared to a snow-covered FYI floe (Sect. 3.3 below).

3.3 Enhancement of seasonal ice melting caused by wave flooding and wave pulverisation

Here we consider the radiative effects of both wave flooding of a single idealised snow-covered floe and wave pulverisation that creates wave slush, in order to compute the increase in the vertical melt rate of wave-flooded and wave-pulverised ice compared to a snow-covered FYI floe. We term this “wave-induced melt-rate enhancement” (see Sect. 2.2). For illustration, we work through an example representing approximately the midpoint of the austral melt season for the approximate middle latitude of the SIZ, namely on the December solstice at 65°S . We initially focus on wave-overwashed ice, wave compression-flooded FYI and wave-pulverised slush, where $\Delta\alpha = 0.38$ (Table 1b), and take f_w (the fraction of floe area affected by wave flooding) to be 1.0. For this example:



(1) On the December solstice at 65°S, the downward shortwave (SW) flux at the top of the atmosphere (F_{TOA}) is 510 W m⁻² (Fig. 2.7 of Hartmann, 2016). This corresponds to an effective daily average solar zenith angle of 68° (solar constant is 1360 W m⁻²; $\cos^{-1}(510/1360) = 68^\circ$).

385 (2) For solar zenith angle 68°, we get the downward SW at the surface, F_{sfc} , as described in Sect. 2.2. The corresponding atmospheric transmittance over sea ice is $t_a = 0.52$, so $F_{sfc} = 0.52 \times 510 = 264 \text{ W m}^{-2}$.

(3) Referring back to Eq. (5), the radiative forcing caused by wave flooding (RF_w) is then:

$$RF_w = \Delta\alpha F_{sfc} = 0.38 \times 264 = \sim 100 \text{ W m}^{-2}.$$

390 (4) To get regional averages, we would multiply RF_w by the ice concentration (C) and the fraction of floe surfaces that are wave flooded or the area of ice that is wave-pulverised (f_w) (see Eq. 6 in Sect. 2.2). However, as we are dealing with an idealised single floe (slab) or idealised mass (small area) of wave slush, C is here to be 1.0 and we can compute the melt-rate enhancement by Eq. (7) (Sect. 2.2).

For this example at 65°S and where $f_w = 1.0$, the estimated wave-driven enhancement in vertical melt rate dh/dt for wave-flooded ice and wave slush (compared to snow-covered FYI) is 2.9 cm day⁻¹.

395 We next carry out a sensitivity analysis of wave-driven enhancements in daily melt rates for the four different wave-affected classes where $\Delta\alpha$ is 0.38, 0.48, 0.54 and 0.64, as a function of: 1) f_w , with values of 0.33 and 0.5 in addition to 1.0 derived from visual inspection of photographs acquired from icebreakers (Fig. 1a–j); 2) latitude; and 3) time of year from November through January (the main period of annual sea-ice retreat). The estimated melt-rate enhancement values for 60°S to 70°S, i.e., the zone typically covered by sea ice during the annual retreat phase (e.g., Massom et al., 2013), are plotted in Fig. 3, while values for the wider latitudinal range of 55–75°S are shown in the Appendix in Tables A1–A3. Over the range of latitudes examined, 400 wave-enhanced rates of ice melt steadily build up through late austral spring (November). Not surprisingly, the lower the latitude, the higher the melt-rate enhancement, and there is strong dependence on f_w , i.e., the greater the fraction of a floe surface that is wave flooded or the area of ice that is wave-pulverised, the higher the melt-rate enhancement. In all cases, the melt-rate enhancement values converge towards a broad annual peak around the December solstice, before slowly decreasing through January (mid-summer).

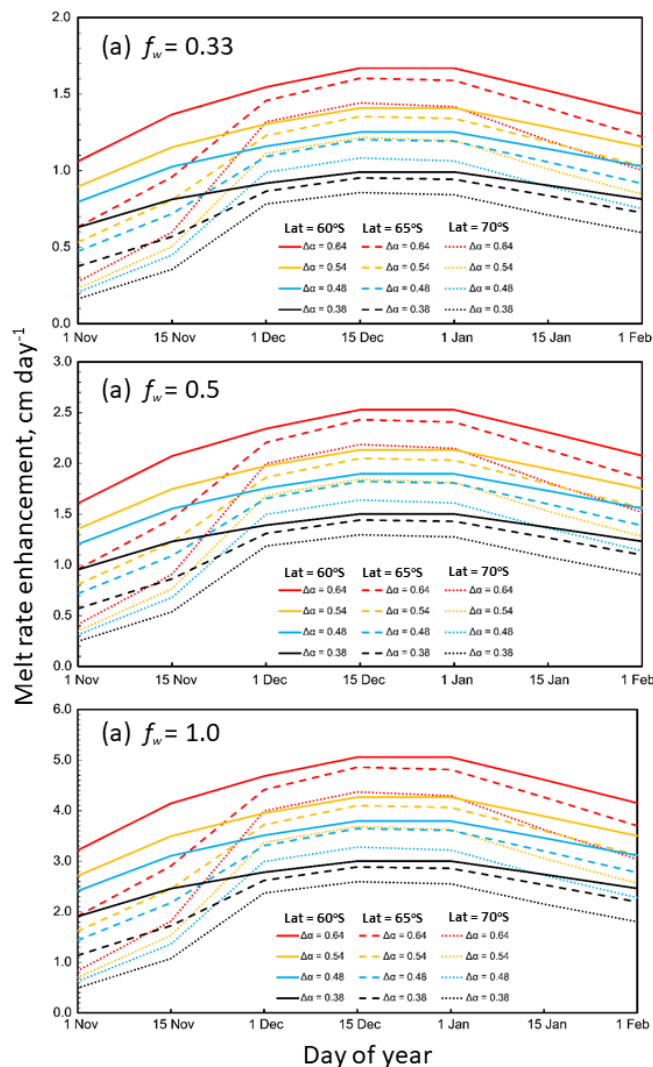


Figure 3: Plots of sea-ice melt-rate enhancement based on albedo change/reduction ($\Delta\alpha$) related to different types of wave flooding and wave pulverisation, as a function of latitude (60°S , 65°S and 70°S), time of year (November through January), and for sea ice of density 905 kg m^{-3} . For a) $f_w = 0.33$; b) $f_w = 0.5$; and c) $f_w = 1.0$. Note the different scales on the y axes. Coincident estimated values of wave-driven melt-rate enhancement for 55°S - 75°S are given in Tables A1-A3.

Annual summer-maximum wave-induced melt rate enhancement values (on 15 December) for the four wave-affected ice-surface type categories, as a function of latitude (60°S , 65°S and 70°S) and f_w (0.33, 0.5 and 1.0), are given in Table 2. For ice-surface types A and C which are unaffected by algae, these range from 0.9 cm day^{-1} (for type A at 70°S where $f_w = 0.33$)



to 4.3 cm day⁻¹ (type C at 60°S where $f_w = 1.0$). Algal greening increases the wave-induced melt-rate enhancement by between 0.2 and 0.8 cm day⁻¹. In all cases, melt-rate enhancement triples when f_w increases from 0.33 to 1.0, and doubles when f_w increases from 0.5 to 1.0. Moreover and for any given wave-affected ice-surface type, there is a slight decrease in the wave-driven melt rate enhancement with increasing latitude south (Tables A1–A3 and Fig. 3), which is greatest in late austral spring (November) compared to summer. Sea-ice coverage south of 70°S is largely confined to the Weddell, Amundsen and Ross seas, whereas sea ice across East Antarctica mainly occurs equatorward of 67°S (Massom et al., 2013). The highest melt-rate enhancements are at 55°S (Tables A1–A3), but sea ice usually attains that latitude only in the eastern limb of the Weddell Gyre at ~5–25°E and parts of East Antarctica around ~80°E, and only in winter through October (cf., Massom et al., 2013).

Wave-affected surface type	Latitude 60° S			Latitude 65° S			Latitude 70° S		
	$f_w = 0.33$	$f_w = 0.5$	$f_w = 1.0$	$f_w = 0.33$	$f_w = 0.5$	$f_w = 1.0$	$f_w = 0.33$	$f_w = 0.5$	$f_w = 1.0$
A, $\Delta\alpha = 0.38$	1.0	1.5	3.0	1.0	1.4	2.9	0.9	1.3	2.6
B, $\Delta\alpha = 0.48$	1.3	1.9	3.8	1.2	1.8	3.6	1.1	1.6	3.3
C, $\Delta\alpha = 0.54$	1.4	2.1	4.3	1.4	2.1	4.1	1.2	1.8	3.7
D, $\Delta\alpha = 0.64$	1.7	2.5	5.1	1.6	2.4	4.9	1.4	2.2	4.4

Table 2. Annual maximum wave-induced sea-ice melt rate enhancement (in cm day⁻¹), on 15 December, for the four wave-affected ice-surface type categories (see Table 1b), as a function of latitude (60°S, 65°S and 70°S) and f_w (0.33, 0.5 and 1.0). Type A is wave-overwashed FYI, wave-compression flooded ice, and/or wave-pulverised slush; B is wave-pulverised slush – green; C is wave pond, and/or wave-deformation pond; and D is wave pond, or bare ice – green. Sea-ice density = 905 kg m⁻³.

The wave-induced melt-rate enhancement values shown in Table 2 are for sea ice with fixed density 905 kg m⁻³ (see Eq. 7), which is taken here to be an approximation of a FYI floe under cold conditions. Although the densities of the four wave-affected ice-surface types are unknown, they may be lower than 905 kg m⁻³ – particularly for wave slush, but also for the other wave-affected surface types shown in Fig. 1 – and progressively become even lower as wave-induced surface and internal ice melting progresses and ice permeability and porosity increase through late-spring and summer. This would be the case if the pore spaces are filled with air, but the density would increase if the pores filled with water. Given these factors and current unknowns, we now investigate the effect of lowering ice density on wave-induced melt-rate enhancement, using a value of 750 kg m⁻³ measured in Lützow-Holm Bay in East Antarctica by Urabe and Inoue (1988). Results are shown in Table 3. These indicate melt-rate enhancements in the range of 1.0 to 6.1 cm day⁻¹ (again depending on surface type, latitude, f_w , and greening), i.e., an increase of between 0.1 and 1.0 cm day⁻¹ compared to ice with density 905 kg m⁻³.



Wave-affected surface type	Latitude 60° S			Latitude 65° S			Latitude 70° S		
	f_w 0.33	f_w 0.5	f_w 1.0	f_w 0.33	f_w 0.5	f_w 1.0	f_w 0.33	f_w 0.5	f_w 1.0
A, $\Delta\alpha = 0.38$	1.2	1.8	3.6	1.1	1.7	3.5	1.0	1.6	3.1
B, $\Delta\alpha = 0.48$	1.5	2.3	4.6	1.5	2.2	4.4	1.3	2.0	4.0
C, $\Delta\alpha = 0.54$	1.7	2.6	5.2	1.6	2.5	4.9	1.5	2.2	4.5
D, $\Delta\alpha = 0.64$	2.0	3.1	6.1	1.9	2.9	5.9	1.7	2.6	5.3

Table 3. Annual maximum wave-induced sea-ice melt rate enhancement (in cm day^{-1}), on 15 December, for the four wave-affected ice-surface type categories (see Table 1b), as a function of latitude (60°S, 65°S and 70°S) and f_w (0.33, 0.5 and 1.0). Type A is wave-overwashed FYI, wave-compression flooded ice, and/or wave-pulverised slush; B is wave-pulverised slush – green; C is wave pond, and/or wave-deformation pond; and D is wave pond, or bare ice – green. Sea-ice density = 750 kg m^{-3} .

4 Discussion

4.1 Melt enhancement by wave flooding and wave pulverisation

Our results indicate that wave flooding and pulverisation exert a strong influence on the vertical melt rate of affected areas of the Antarctic SIZ in summer, and highlight the need for detailed large-scale measurements, *in situ* observations, mapping and numerical modelling. We highlight that wave-flooded and wave-pulverised regions of the outer MIZ will have little or no snow cover during the summer melt season. This also applies to sea ice immediately adjacent to polynyas and large leads within the interior SIZ (due to the occurrence of wind waves there), but contrasts with other areas of the interior SIZ, where snow cover may persist during summer (Massom et al., 2001). Depending on the wave-process type, it is estimated that wave flooding and wave pulverisation reduce the albedo of typical FYI >0.7 m thick by 0.38–0.54, or by 0.28–0.44 for <0.7 m-thick ice, where the reductions are compared to snow-covered ice (Table 1). These values increase by an estimated 0.1 to 0.48–0.64 and 0.38–0.54, respectively, due to rapid greening of the ice (again driven by wave flooding and wave pulverisation).

These large albedo reductions substantially increase the absorption of solar radiation by the wave-affected floes and wave slush as insolation increases following the September equinox, and within the annual window of most Antarctic sea-ice melting, i.e., November–December–January. At its mid-December maximum and depending on (i) wave-affected surface type, (ii) fraction of the floe/surface affected, (iii) latitude (over the range 60–70°S) and (iv) ice density (here 750 or 905 kg m^{-3}), the estimated increase in vertical melting due to wave flooding and/or wave pulverisation and compared to snow-covered FYI ranges from 0.9 cm day^{-1} to 5.2 cm day^{-1} (Tables 1 and 2). This range of wave-induced melt-rate enhancement increases to 1.1 cm day^{-1} to 6.1 cm day^{-1} for wave-affected surface types darkened by algae. Note that these estimates of melt-rate enhancement are instantaneous, and do not consider non-linear feedbacks over time that result from the increased melt driven



by wave processes (see Sect. 4.3). Estimating additional melt-rate enhancements due to feedbacks is outside the scope of this paper, but is worthy of investigation. Another factor that may further enhance ice interior melting is the absorption of incoming solar radiation by ice algae proliferating in the wave-affected ice habitat, due to their pigmentation (cf., Zeebe et al., 1991).

Our computation indicates that, all else being equal, albedo reduction by wave flooding or wave pulverisation (and wave greening) could cause a 1-m-thick floe or mass of wave slush to absorb enough additional solar energy to melt away in just one month – although again this rate may accelerate over time due to melt-related non-linear feedbacks outlined below (Sect. 4.3). This wave-induced surface melting is in addition to, and supplements, ice-floe lateral and basal melting (not considered here). While there is large uncertainty in these first-approximation estimates due to lack of observations, they indicate a strong need to investigate wave-melting processes towards their inclusion in sea-ice, climate and Earth-system models.

Although outside the scope of this initial study, it is likely that wave-flooding and wave-pulverisation processes further contribute to seasonal sea-ice melting in two additional ways, and that a third process affects the exact location of the melting in the floe, i.e., whether it occurs in the ice interior or instead on the floe base and sides. First, wave overwashing and flooding likely make a direct contribution to ice-surface melting where the sea-surface temperature (SST) rises above $\sim 0^{\circ}\text{C}$ in summer (sea ice has a lower salinity than seawater, which freezes at about -1.8°C). This would be the case for small floes swept northwards from the pack-ice zone into warmer waters by wind-driven Ekman divergence and/or ocean eddies, including within bands.

Second, removal of the insulating snow buffer by waves directly exposes bare floe surfaces and/or wave slush to air temperatures above 0°C as summer progresses. More ephemeral and localised/regional surface melting also occurs in other seasons in the MIZ due to episodic incursions of warm (above-freezing) air temperatures associated with the passage of storms, e.g., even in winter at the relatively-low latitudes attained by the MIZ (Massom et al., 1997), with wave flooding and snow removal again facilitating such melting.

A third factor is the transmission of solar radiation through the ice. This transmission is small for snow-covered floes, but is significant for wave-overwashed bare ice, wave-ponded ice and wave slush. Although no Antarctic measurements are available, Arctic observations show that freshwater melt ponds there increase the amount of shortwave radiation transmitted through the ice in summer by up to about a factor of four (Nicolaus et al., 2012; Light et al., 2015). Arctic melt-pond transmittance attains values of 0.5 compared to ~ 0.2 for bare ice and $\sim 0.0\text{--}0.1$ for snow-covered ice (Perovich, 2005), leading to melt rates under ponds that are 2–3 times higher than they are for bare ice (Fetterer and Untersteiner, 1998). While Arctic-like melt ponds are extremely rare on Antarctic sea ice, wave ponds form a pseudo year-round equivalent in that they act as mini “skylights” that preferentially transmit solar radiation and heat to the floe interior and underlying mixed layer. Increased transmittance of solar radiation through wave flooding might be a key driver for the onset of phytoplankton growth in the ice-covered Southern Ocean (cf., Hague and Vichi, 2021).



Another factor highlighted by this study is that the mechanical break-down of floes in the MIZ occurs not only by wave-driven flexural fracture (Williams et al., 2013) but also by the wave-induced pulverisation of floes and their snow cover into icy slush and small brash-ice fragments (Massom et al., 2006). As a result, low-albedo wave slush can form a significant proportion of the sea-ice cover in the outer MIZ, as shown in Fig. 1i,j. This scenario challenges the commonly-held view that the MIZ is simply a collection of wave-fractured small floes that decrease in size with increasing proximity to the ice edge (open ocean) and are either closely packed or separated by open water (depending on wind direction) – with implications for modelling the seasonal meltback of the ice cover. Moreover, it is likely that unconsolidated fields of wave slush particles and brash-ice fragments are susceptible to particularly rapid seasonal melting due to their small size and their direct contact with wave-induced pulsations of warm seawater in summer – with this melt enhancement being increased by algal greening (Massom et al., 2006).

4.2 Spatio-temporal influence of wave flooding, greening and melting

Due to the current lack of observations, we have not attempted to quantify the overall areal occurrence and influence of wave melting. Despite this caveat, there are a number of key factors to consider, that point to wave melting likely making a substantial contribution to Antarctica's rapid climatological sea-ice seasonal retreat phase when combined and integrated over the entire SIZ. Not least is the vast circumpolar extent of the MIZ (Brouwer et al., 2022; Day et al., 2024) and its constant interaction with both large ocean swells (cf., Young et al., 2020) and wind waves locally generated by intense cyclones (Vichi et al., 2019; Alberello et al., 2022).

Wave melting is not confined to the MIZ. It also occurs more deeply within the SIZ, due to the presence there of large leads and both coastal and offshore polynyas (cf., Barber and Massom, 2007) that are affected by wind waves. It is again likely that the influence of wind-wave driven melting in the interior pack increases as open-water areas within the SIZ expand and remain ice-free as the melt season progresses (cf., Massom et al., 2003). We apply the term “rotting from within” to the large-scale seasonal melting of the interior and coastal SIZ (after Massom et al., 2003). In addition, deep-swell penetration events can drive wave flooding in the interior Antarctic pack. In an example from the Weddell Sea in winter 1986, a series of waves of 18 s period and 1 m amplitude were observed to break up the ice (concentration 90% and average thickness 0.8 m) and cause active rafting and ridging at 560 km in from the ice edge (Liu and Mollo-Christensen, 1988). Also, wave-compression flooding has been observed in the compact inner pack-ice zone up to 360 km south of the East Antarctic sea-ice edge, e.g., Fig. 1g,h (also, cf., Massom et al., 1999).

For compact ice-edge zones, e.g., due to on-ice winds (Massom et al., 2008) with a high concentration of FYI floes, attenuation of incoming wave energy by the ice cover (e.g., Squire 2020) is likely to limit overwashing to a relatively short distance in from the ice edge (Pitt et al., 2022). However, the Antarctic ice-edge zone is typically more diffuse (e.g., see Fig. 1 of Massom and Stammerjohn, 2010) due to the frequent passage of storms (cf., Simmonds et al., 2003) and the occurrence of ocean eddies there (cf., Auger et al., 2023; see also Fig. 9 of Massom et al., 1999) – including in late spring through summer. For the ice-



edge zone, the areal influence of wave flooding, wave pulverisation, wave greening and resultant wave melting is likely extended by the widespread occurrence of extensive fields of bands of floes that peel away from the main SIZ and are separated by areas of open water (Comiso et al., 1992; Wadhams, 2000; Ishida and Ohshima, 2009). Reported widths of Antarctic ice-edge band zones range from about 100 km (Saiki and Mitsudera, 2016) to >300 km (Massom and Stammerjohn, 2010). The percentage coverage of wave overwashing and ponding is particularly high in such bands, e.g., ~50–60% in the narrow band in Fig. 1d.

Two other factors likely enhance the areal occurrence and influence of wave flooding and wave melting around Antarctica. Firstly, Antarctic first-year and younger floes are relatively thin and typically have a near-zero or negative freeboard (Worby et al., 1998; see also Fig. 1b). Secondly, the wave flooding processes themselves can directly contribute to lowering the freeboard (and increasing wave overwashing) by changing the floe isostasy via (i) the creation of raised rims by wave buffeting (Fig. 1c,d; Fig. 2d), (ii) wave-driven deformation processes (see Sect. 3.1.3 and Fig. 1e,f), and (iii) the additional weight of pooled seawater (Fig. 1c-f).

4.3 Positive feedback mechanisms

We propose that wave flooding and pulverisation processes activate three coupled dynamic–thermodynamic positive feedback mechanisms that likely accelerate the rate of ice melt, and also an embedded fourth coupled physical–biological feedback involving the impact of ice-algal pigments (chlorophyll and also accessory photosynthetic and non-photosynthetic algal pigments) on the ice albedo. These feedback mechanisms, which are depicted schematically in Fig. 4–6, have been largely unconsidered to date (cf., Goosse et al., 2018), but merit further investigation towards their inclusion in sea-ice and climate models. All four mechanisms are closely linked and operate in concert, as discussed below.

Firstly, the wave-induced reduction in ice-surface albedo activates a positive sea ice-albedo feedback (Fig. 4) similar/equivalent to that associated with freshwater melt ponds on Arctic sea ice in summer (cf., Curry et al., 1995; Perovich et al., 2009), but in this case involving saline wave ponds, wave-washed bare ice and/or wave-pulverised slush and brash-ice fragments. By this mechanism, the wave-driven decrease in ice-surface albedo increases the absorption of solar radiation and melting, which further reduces the ice albedo, leading to enhanced melting – an amplifying cycle. We also propose that this *wave-driven ice-albedo feedback* is strengthened in places by the additional decrease in albedo associated with the rapid proliferation of ice algae in the high-light and high-nutrient environment of (i) wave-modified floe surfaces (including saline wave ponds) and/or interiors and (ii) wave slush. This greening (increased ice algal pigment content) further enhances the melting of wave-flooded floes and wave slush and represents a *coupled biophysical ice–albedo feedback* or *ice–algae–albedo feedback* (Fig. 4). At the same time, heating of the ocean mixed layer by shortwave radiation transmitted through wave-flooded and wave-ponded ice skylights likely amplifies the open water–sea ice feedback associated with solar heating in leads (cf., Nihashi and Ohshima, 2001), as is the case for melt ponds in the Arctic (Inoue et al., 2008).

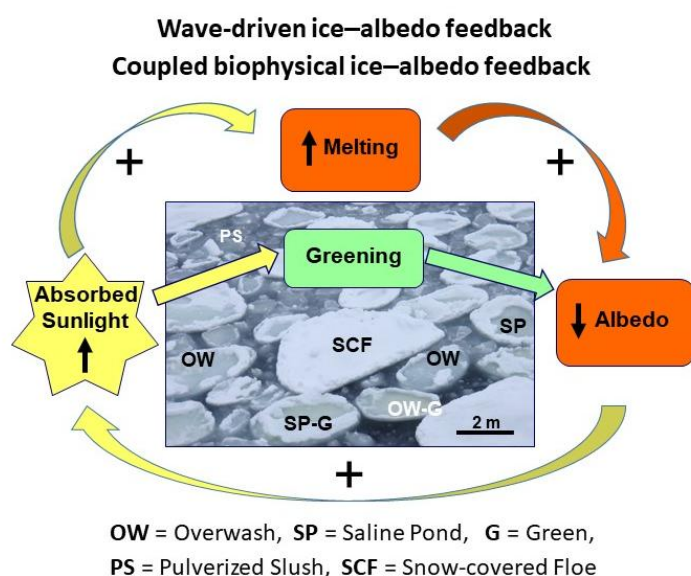
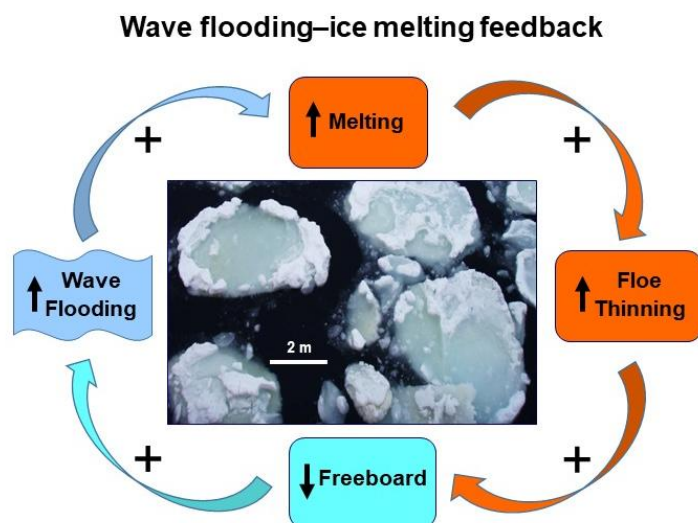


Figure 4: Schematic representation of wave-driven sea ice-albedo feedback, intensified by floe greening, i.e., an embedded coupled biophysical ice-albedo feedback. Up arrows denote an increase, and down arrows a decrease.

560 We also propose that the thinning of small floes by wave melting decreases their freeboard, to increase their susceptibility to further flooding by overwashing and deformation ponding (due to increased rafting with the thinner ice) – thereby increasing the melt-rate enhancement due to wave flooding (see Sect. 3.3 and 4.1), and so on (Fig. 5). This entails a *wave flooding–ice melting feedback*. Concurrently, wave melting also likely increases the ice porosity and permeability. The thinning and increase in ice porosity would together reduce the mechanical strength of floes, i.e., their resistance to compressive and flexural

565 failure (cf., Eicken et al., 1991; Timco and Weeks, 2010), making them more susceptible/vulnerable to further fragmentation by wave flexure into smaller floes – to increase wave flooding and wave melting, leading to further thinning and overwashing, and so on. This represents a *wave flooding–floe fragmentation/breakup feedback* (Fig. 6). This feedback is based on the positive relationship between the strength of a sea-ice “slab” and its thickness (Chai et al., 2021) and the negative relationship between strength and porosity (Timco and Weeks, 2010; Wang et al., 2022; Mellor, 1986; Eicken et al., 1991). Moreover,

570 smaller floes are more mobile and more likely to peel away in bands and/or drift northwards and away from the main pack under Ekman divergence driven by the prevailing westerly winds and/or ocean eddies (cf., Auger et al., 2023), i.e., into warmer waters where they rapidly melt.



575 **Figure 5:** Schematic representation of wave flooding–ice melting feedback. Up arrows denote an increase, and down arrows a decrease.

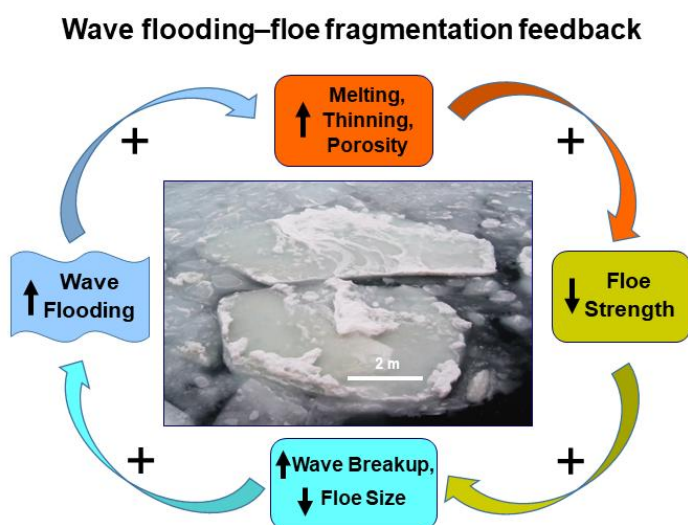


Figure 6: Schematic representation of wave flooding–floe fragmentation feedback. Up arrows denote an increase, and down arrows a decrease.

580 The wave-driven *ice-algae-albedo feedback* is likely intensified by an increase in ice porosity and permeability due to increased absorption and transmittance of solar radiation, and its conversion to heat, by algae embedded in the ice structure (cf., Zeebe



et al., 1996). This would then stimulate additional ice-algal growth by facilitating nutrient replenishment and algal transport through the more permeable ice column – to further enhance the coupled biophysical ice–albedo feedback. At the same time, the algae–permeability sub-feedback and wave-induced greening likely intensify the wave flooding–floe fragmentation feedback, by further decreasing the mechanical strength of the small floes (cf., Eicken et al., 1991). These feedbacks also enhance the ocean–ice albedo feedback (i.e., floe lateral and basal melting, cf., Nihashi and Cavalieri, 2006) by creating smaller floes that are more mobile than large floes and have a larger perimeter per unit area. Any decrease in sea-ice density due to wave flooding, wave pulverisation and wave greening would increase the sea-ice melt rate (dh/dt) due to radiative forcing (see Eq. 7).

5 Conclusions and outlook

We have built on the classical picture of seasonal melting of Antarctic sea ice each October to February due to lateral and basal melting which are accelerated by a positive ocean–ice albedo feedback (e.g., Horvat, 2022) accentuated by the wave-driven breakup of floes in the MIZ. We have provided evidence that waves also drive a suite of previously-neglected coupled dynamic–thermodynamic processes (termed wave flooding and wave pulverisation) that remove the thermal and optical buffer provided by snow cover – not only in the MIZ but also in the interior SIZ where wind waves prevail. These wave-driven processes reduce the sea-ice albedo by up to an estimated 0.54 compared to snow-covered ice, thereby increasing the absorption of solar radiation by the ice and generating (previously neglected) rapid surface and interior melting of both floes and wave slush (previously neglected) in summer. This additional melting is amplified by an estimated additional decrease of 0.1 in ice albedo due to a proliferation of ice algae (greening) in the high-light and high-nutrient sea-ice habitats created by wave flooding and wave pulverisation.

Further, we propose that wave flooding and wave pulverisation activate four previously-unconsidered coupled dynamic–thermodynamic positive feedbacks that link sea-ice physics to biology – and that these feedbacks likely result in additional acceleration of seasonal sea-ice melting to contribute to the rapid climatological melt phase of Antarctica’s annual sea-ice cycle. In the warm season, the increase in through-ice transmittance of solar radiation due to the wave flooding, wave pulverisation and wave greening also likely contributes to heating the ocean mixed layer (cf., Nicolaus et al., 2010). This would further enhance basal and lateral melting (due to absorption of sunlight in leads and polynyas), to strengthen the more generally considered open ocean–ice albedo feedback (cf., Goosse et al., 2018). The complex wave-melting feedbacks and non-linear relationships identified in this study require and warrant further analysis towards their inclusion in models, as they have implications for 1) accelerating sea-ice loss while also enhancing climate warming, 2) attributing observed recent high variability, and 3) predicting future climate, sea-ice conditions and impacts. Also worthy of investigation is the effect of wave melting on freshwater input into the ocean, with implications for upper-ocean stratification that may enhance ice formation – and potential feedbacks involved.



Ice-edge bands have been considered to influence the seasonal evolution of the MIZ, e.g., in the Arctic (Martin et al., 1983), by increasing the open-water area within the pack and promoting rapid lateral and basal melting of floes within the outer MIZ (Saiki and Mitsudera, 2016). To this, we add the influence of wave melting processes on floes within the bands themselves, and hypothesize that bands (and ice-edge ocean eddies) play an important role in extending the spatial domain of wave-melting influence – including smaller bands such as that in Fig. 1d. More work is required to investigate and quantify this factor, and to determine how banding distribution, composition (floe size) and processes interact with waves, and how bands respond to changing wind and wave conditions under a warming climate – and how this will influence wave flooding and melting.

By generating elevated concentrations of ice algae compared to snow-covered floes, wave flooding and wave pulverisation contribute to another positive feedback involving sea-ice biological and biogeochemical cycles. In spring–summer, ice algae (and phytoplankton blooms in the ocean as the ice melts back in summer) produce dimethylsulfoniopropionate, a precursor of the gas dimethyl sulfide, which gets oxidised in the atmosphere to form sulfate particles which in turn serve as cloud-condensation nuclei. Clouds formed in this way then influence the surface radiation and energy balances (Tison et al., 2017) and precipitation – to affect sea-ice conditions and algal production, and so on (cf., Charlson et al., 1987; Wang et al., 2018). The complex relationships between wave flooding, wave melting and wave pulverisation, coupled physical–biological–biogeochemical processes and cloud physics are outside the scope of this paper, but again require and warrant detailed investigation with targeted cross-disciplinary observations and modelling that we hope are stimulated by this paper.

Wave-flooded floes and wave slush form “mini oases” and hotspots respectively for enhanced primary productivity. This results in extensive intra-ice algal blooms relatively early in the season compared to open-ocean phytoplankton blooms, and that are undetected in satellite ocean-colour datasets (Massom et al., 2006). Wave flooding and wave pulverisation also likely contribute to supporting active algal communities and elevated chlorophyll concentrations in low-light-level months before the September equinox, including those observed in the winter Antarctic MIZ (cf., Louw et al., 2022) when the ice reaches relatively low latitudes of ~57°S–60°S in places. Given these factors, we hypothesise that wave flooding and wave pulverisation make previously-neglected contributions to: 1) overall year-round primary production within the Antarctic SIZ (cf., Saenz and Arrigo, 2014; Dalman et al., 2025) including the MIZ (cf., Taylor et al., 2013); 2) phytoplankton blooms under sea ice (cf., Hague and Vichy, 2021; Horvat et al., 2022); and 3) phytoplankton blooms in late-spring through summer both seaward of the ice edge as it retreats (Massom et al., 2006; cf., Arrigo et al., 2014; Ito et al., 2025) and within polynyas (cf., Arrigo and van Dijken, 2003). This has implications for the uptake by the Southern Ocean of anthropogenic carbon from the atmosphere, the biological carbon pump (Henley et al., 2020), and the ocean’s moderation of climate warming (cf., Frölicher et al., 2015). At the same time, wave flooding and wave pulverisation likely increase the release of algae and biogenic material into the upper ocean and its availability for under-ice pelagic grazers in the MIZ year round and at the receding ice edge in late spring–summer, which then support higher trophic levels (Massom et al., 2006).

On the small scale, it is likely that wave flooding and melting processes substantially modify the microstructure and mechanical properties of sea-ice floes, by progressively increasing the sea-ice porosity and permeability, decreasing its density and



645 changing its salinity, brine volume and temperature (cf., Golden et al., 1998). In terms of computations of melt-rate
enhancement (see Eq. 7), the densities of wave-flooded, wave-pulverised and wave greened-ice – and their evolution as the
melt season progresses – represent a major current unknown, and may be lower than the densities of 905 kg m^{-3} and even 750
 kg m^{-3} used in Eq. (7). This factor, in concert with the additional vertical melt-rate enhancements by the four newly-proposed
positive feedback mechanisms driven by wave flooding and wave pulverization, means that the melt-rate enhancement
650 estimates provided here may in fact be underestimates. An additional unknown, outside the scope of this analysis, is the
magnitude of the contribution of wave flooding to ice-floe lateral and basal melting, and the associated ocean–ice albedo
feedback (cf., Nihashi and Cavalieri, 2006).

Wave flooding and wave pulverisation also have implications for the retrieval of sea-ice concentration (and extent) from
satellite passive-microwave brightness temperature data (Massom et al., 1999; and cf., Comiso et al., 1992 and Ivanova et al.,
655 2015). For example, the ice covers shown in Fig. 1a, Fig. 1g and Fig. 1i have a 100% concentration, but this value is likely to
be substantially underestimated in satellite passive-microwave products as the microwave emissivity of flooded ice and/or
wave slush is intermediate between that of snow-covered dry ice and open water (cf., Comiso and Steffen, 2001). In addition,
wave flooding and wave pulverisation have implications for the accurate estimation of both sea-ice and snow-cover thickness
from satellite radar and laser altimeter measurements (cf., Kacimi and Kwok, 2020), and are factors that need accounting for
660 (certainly in Antarctica’s extensive circumpolar MIZ).

In the Arctic, there has been strong recognition of the need for explicit treatment of melt ponds in models (e.g., Taylor and
Feltham, 2004; Flocco et al., 2010; Tsamados et al., 2015; Webster et al., 2022), in order to simulate both Earth’s radiation
balance (Maslanik et al., 2007; Perovich et al., 2008; Nicolaus et al., 2010) and the strength of the ice–albedo feedback (Curry
et al., 1995, 2001; Tschudi et al., 2008). This same recognition is required for wave-washed floes, saline wave ponds and
665 wave-pulverised slush in the Antarctic (and the Arctic), all modulated by additional albedo changes due to associated ice-algal
greening – albeit on a smaller scale given the lower proportional coverage compared to summer melt ponds in the Arctic.
However, there are fundamental differences. Unlike Arctic melt ponding that only occurs in the melt season, wave-flooding
and wave-pulverisation processes and associated snow removal occur year round. They exert year-round influence on the
energy budget and mass balance of the SIZ, and also have implications for the ocean freshwater budget and upper-ocean
670 buoyancy and stratification.

Given the factors highlighted in this paper, it is likely that wave-melting processes contribute to: 1) the predominant role of
the MIZ in driving overall mean annual sea-ice retreat around Antarctica (cf., Kimura et al., 2022); and 2) the observed close
spatio-temporal correspondence between (trends in) significant wave height and circum-Antarctic sea-ice extent and annual
retreat identified by Kohout et al. (2014). We support their assertion that Antarctic sea ice is vulnerable to increased storminess,
675 and add wave flooding, greening, pulverisation and melting to wave fragmentation as key processes affecting sea-ice seasonal
melting. Moreover, while our focus has been on Antarctic sea ice, wave-flooding, wave-pulverisation and wave-melting



processes and associated feedback mechanisms also apply to the Arctic (e.g., Massom, 1991) – and to not only marginal seas but also the central Arctic Ocean where wave-ice interaction processes occur.

Wave flooding may already be intensifying, given observed increases in recent decades in: (i) cyclones at high southern
680 latitudes related to a poleward shift in storm tracks (IPCC, 2014), and (ii) both wave height and near-surface wind speed over the Southern Ocean adjacent to the SIZ (Young and Ribal, 2019; Morim et al., 2019). In the Northern Hemisphere, loss of sea-ice coverage (particularly in summer, e.g., Comiso et al., 2017b) has exposed the Arctic Ocean to more swells (Thomson and Rogers, 2014) to increase the likelihood of more extensive wave flooding, pulverisation and melting there.

Looking to the future and for Antarctica, wave flooding, wave pulverisation and wave melting processes – in harness with the
685 associated feedbacks identified above – have the potential to increase in their areal extent and influence in coming decades, given predicted further increases in wind speed and wave height across the high-latitude Southern Ocean (Casas-Prat et al., 2024). This intensification would contribute to changing Antarctic sea-ice formation and melt rates, and the thickness and properties of the ice and its snow cover (cf., Webster et al., 2018). In turn, these changes have major implications for: the extent and seasonal duration of the seasonal pack-ice zone (cf., Stammerjohn et al., 2012) and the coastal fast-ice zone (cf.,
690 Fraser et al., 2023); planetary albedo and Earth's surface energy and heat budgets (cf., Riihelä et al., 2021), with a decrease in albedo due to wave-driven snow loss and sea-ice modification (and loss) amplifying the positive contribution to the climate feedback at high southern latitudes (cf., Williams et al., 2023); oceanic and atmospheric interactions, properties and circulation, and the global freshwater budget (cf., Haumann et al., 2016; Meredith and Brandon, 2017; Smith et al., 2017; England et al., 2018); low-latitude and global weather and climate (cf., England et al., 2020; Ayres et al., 2022); the stability of the Antarctic
695 ice shelves, ice-sheet mass loss and sea-level rise (cf., Massom et al., 2018; Teder et al., in press); primary production both within and under the ice, habitat quality, krill and food-web energetics, and marine ecosystem health and biodiversity (cf., Massom and Stammerjohn, 2010; Ducklow et al., 2013; Meredith et al., 2019); the critical capacity of the Southern Ocean to take up atmospheric carbon and to moderate anthropogenic climate change (cf., Williams et al., 2023), while also influencing ocean acidification (cf., Nissen et al., 2024); and important biogeochemical processes that feed back into the climate system
700 (cf., Vancoppenolle et al., 2013).

6 Recommendations for needed measurements and work

As stated in the Introduction, the new paradigms presented here are based on limited observations and simple modelling. An important next step is to carry out targeted measurements, both large-scale and small-scale, in order to quantify and more fully understand wave flooding, wave pulverisation, wave greening and wave melting – and the associated feedbacks identified –
705 as a function of space and time, and their relationship to wave and ice conditions, including floe size; distance from the ice edge; ice type and thickness; and banding. Obtaining estimates of these quantities and of f_w and C in Eq. 6, and their seasonal and spatial variations is challenging, given the scale and dynamism of the environment involved. It will require coordinated use of autonomous technologies – such as ship-borne stereo camera systems (e.g., Alberello et al., 2022), wave and ice mass-



balance buoys, and drone remote sensing including hyperspectral sensors to detect and quantify greening – extended in space
 710 and time using satellite remote sensing (e.g., ultra-high-resolution) and combined with novel altimetric measurement of wave
 penetration distances into the SIZ (e.g., Brouwer et al., 2022; Fraser et al., in prep.). Ship-based and *in situ* spectral radiation
 measurements are needed for the albedo and transmittance of the different wave-affected surfaces, including the effect of algal
 greening on albedo. Also needed are coincident detailed *in situ* observations of the morphology, density and micro-structural
 properties of wave flooded and wave-pulverised ice, and their algal pigment content and composition, primary production and
 715 nutrients; and production of climate-active gases by wave-affected ice. In parallel, dedicated modelling efforts are required to
 synthesise the observations and carry out detailed sensitivity analyses. There is compelling need to work on including these
 important wave-melting processes and feedbacks in coupled models, as a crucial step towards 1) the more accurate simulation
 of the annual cycle of Antarctic sea ice and its current state, and 2) more robust predictions of the future fate of both polar sea-
 ice systems and the wider Earth system.

720 7 Appendix

$\Delta\alpha = 0.64$	1 Nov	15 Nov	1 Dec	15 Dec	1 Jan	15 Jan	1 Feb
55°S	1.2	1.5	1.6	1.7	1.7	1.5	1.5
60°S	1.1	1.4	1.5	1.7	1.7	1.5	1.4
65°S	0.6	1.0	1.5	1.6	1.6	1.4	1.2
70°S	0.3	0.6	1.3	1.4	1.4	1.2	1.0
75°S	0.2	0.6	1.3	1.5	1.5	1.3	1.0
$\Delta\alpha = 0.54$	1 Nov	15 Nov	1 Dec	15 Dec	1 Jan	15 Jan	1 Feb
55°S	1.1	1.3	1.3	1.5	1.5	1.3	1.2
60°S	0.9	1.2	1.3	1.4	1.4	1.3	1.2
65°S	0.5	0.8	1.2	1.4	1.3	1.2	1.0
70°S	0.2	0.5	1.1	1.2	1.2	1.0	0.8
75°S	0.1	0.5	1.1	1.2	1.3	1.1	0.8
$\Delta\alpha = 0.48$	1 Nov	15 Nov	1 Dec	15 Dec	1 Jan	15 Jan	1 Feb
55°S	0.9	1.1	1.2	1.3	1.3	1.2	1.1
60°S	0.8	1.0	1.2	1.3	1.3	1.1	1.0
65°S	0.5	0.7	1.1	1.2	1.2	1.1	0.9
70°S	0.2	0.4	1.0	1.1	1.1	0.9	0.8
75°S	0.1	0.5	1.0	1.1	1.1	1.0	0.7
$\Delta\alpha = 0.38$	1 Nov	15 Nov	1 Dec	15 Dec	1 Jan	15 Jan	1 Feb
55°S	0.7	0.9	0.9	1.0	1.0	0.9	0.9
60°S	0.6	0.8	0.9	1.0	1.0	0.9	0.8
65°S	0.4	0.6	0.9	1.0	0.9	0.8	0.7
70°S	0.2	0.4	0.8	0.9	0.8	0.7	0.6
75°S	0.1	0.4	0.8	0.9	0.9	0.8	0.6

Table A1. Estimated values of vertical melt-rate enhancement (in cm day^{-1}) for the four wave-affected classes where $f_w = 0.33$, as a function of change in albedo ($\Delta\alpha = 0.64, 0.54, 0.48$ and 0.38), latitude (55°S - 75°S) and time (1 November-1 February). Sea-ice density = 905 kg m^{-3} . Values for 60°S , 65°S and 70°S are plotted in Figure 3a.



$\Delta\alpha = 0.64$	1 Nov	15 Nov	1 Dec	15 Dec	1 Jan	15 Jan	1 Feb
55°S	1.9	2.3	2.4	2.6	2.6	2.3	2.2
60°S	1.6	2.1	2.3	2.5	2.5	2.3	2.1
65°S	1.0	1.5	2.2	2.4	2.4	2.1	1.8
70°S	0.4	0.9	2.0	2.2	2.1	1.8	1.5
75°S	0.3	1.0	2.0	2.2	2.3	2.0	1.5
$\Delta\alpha = 0.54$	1 Nov	15 Nov	1 Dec	15 Dec	1 Jan	15 Jan	1 Feb
55°S	1.6	1.9	2.0	2.2	2.2	2.0	1.9
60°S	1.4	1.7	2.0	2.1	2.1	1.9	1.8
65°S	0.8	1.2	1.9	2.1	2.0	1.8	1.6
70°S	0.4	0.8	1.7	1.8	1.8	1.5	1.3
75°S	0.2	0.8	1.7	1.9	1.9	1.7	1.3
$\Delta\alpha = 0.48$	1 Nov	15 Nov	1 Dec	15 Dec	1 Jan	15 Jan	1 Feb
55°S	1.4	1.7	1.8	2.0	2.0	1.8	1.7
60°S	1.2	1.6	1.8	1.9	1.9	1.7	1.6
65°S	0.7	1.1	1.7	1.8	1.8	1.6	1.4
70°S	0.3	0.7	1.5	1.6	1.6	1.4	1.1
75°S	0.2	0.7	1.5	1.7	1.7	1.5	1.1
$\Delta\alpha = 0.38$	1 Nov	15 Nov	1 Dec	15 Dec	1 Jan	15 Jan	1 Feb
55°S	1.1	1.3	1.4	1.5	1.5	1.4	1.3
60°S	1.0	1.2	1.4	1.5	1.5	1.4	1.2
65°S	0.6	0.9	1.3	1.4	1.4	1.3	1.1
70°S	0.2	0.5	1.2	1.3	1.3	1.1	0.9
75°S	0.2	0.6	1.2	1.3	1.3	1.2	0.9

725 **Table A2.** Estimated values of vertical melt-rate enhancement (in cm day^{-1}) for the four wave-affected classes where $f_w = 0.5$, as a function of change in albedo ($\Delta\alpha = 0.64, 0.54, 0.48$ and 0.38), latitude (55°S - 75°S) and time (1 November-1 February). Sea-ice density = 905 kg m^{-3} . Values for 60°S , 65°S and 70°S are plotted in Figure 3b.



$\Delta\alpha = 0.64$	1 Nov	15 Nov	1 Dec	15 Dec	1 Jan	15 Jan	1 Feb
55°S	3.8	4.5	4.8	5.2	5.2	4.7	4.4
60°S	3.2	4.1	4.7	5.1	5.1	4.6	4.1
65°S	1.9	2.9	4.4	4.9	4.8	4.3	3.7
70°S	0.8	1.8	4.0	4.4	4.3	3.6	3.0
75°S	0.5	1.9	4.1	4.4	4.5	4.0	3.0
$\Delta\alpha = 0.54$	1 Nov	15 Nov	1 Dec	15 Dec	1 Jan	15 Jan	1 Feb
55°S	3.2	3.8	4.1	4.4	4.4	4.0	3.8
60°S	2.7	3.5	4.0	4.3	4.3	3.9	3.5
65°S	1.6	2.5	3.7	4.1	4.1	3.6	3.1
70°S	0.7	1.5	3.4	3.7	3.6	3.1	2.6
75°S	0.4	1.6	3.4	3.7	3.8	3.4	2.6
$\Delta\alpha = 0.48$	1 Nov	15 Nov	1 Dec	15 Dec	1 Jan	15 Jan	1 Feb
55°S	2.8	3.4	3.6	3.9	3.9	3.5	3.3
60°S	2.4	3.1	3.5	3.8	3.8	3.5	3.1
65°S	1.4	2.2	3.3	3.6	3.6	3.2	2.8
70°S	0.6	1.4	3.0	3.3	3.2	2.7	2.3
75°S	0.4	1.4	3.0	3.3	3.4	3.0	2.3
$\Delta\alpha = 0.38$	1 Nov	15 Nov	1 Dec	15 Dec	1 Jan	15 Jan	1 Feb
55°S	2.2	2.7	2.9	3.1	3.1	2.8	2.6
60°S	1.9	2.5	2.8	3.0	3.0	2.7	2.5
65°S	1.1	1.7	2.6	2.9	2.9	2.5	2.2
70°S	0.5	1.1	2.4	2.6	2.6	2.2	1.8
75°S	0.3	1.1	2.4	2.6	2.7	2.4	1.8

730 **Table A3.** Estimated values of vertical melt-rate enhancement (in cm day^{-1}) for the four wave-affected classes where $f_w = 1.0$, as a function of change in albedo ($\Delta\alpha = 0.64, 0.54, 0.48$ and 0.38), latitude (55°S - 75°S) and time (1 November-1 February). Sea-ice density = 905 kg m^{-3} . Values for 60°S , 65°S and 70°S are plotted in Figure 3c.

8 Code availability

To be provided.

735 9 Data availability

To be provided.

10 Author contribution

RAM conceptualised the study and carried out the observations. SGW, BL and DKP provided albedo data, SGW designed the surface radiation energy budget calculation, PAR developed the model code and ran the model, and RAM and PAR
740 analysed the output. LGB, MHM, AT and GP provided expert input on wave-ice interaction; PU, SPO, PAR and PGS on sea-ice modelling; KMM, PGS and PW on sea-ice algae; and ADF, PW, SC and MF on remote sensing. RAM prepared the manuscript with contributions from all co-authors.



11 Competing interests

KM is a member of the editorial board of The Cryosphere.

745 12 Acknowledgements

RM is very grateful to the Australian, US and German Antarctic programs and the masters and crews of the icebreakers RVs *Aurora Australis*, *Nathaniel B Palmer* and *Polarstern*, and to Drs Ray Smith and Sharon Stammerjohn for enabling his participation in the US National Science Foundation Palmer LTER program. SGW thanks the Institute for Marine and Antarctic Studies (IMAS) for their hospitality during visits to Hobart to work on this paper. We gratefully acknowledge the
750 US National Snow and Ice Data Center for the satellite sea-ice concentration data used in this study.

13 Financial support

This work was funded by, and contributes to, Australian Antarctic Science Projects 189, 741, 4073, 4116, 4123, 4298, 4625 and 4635. For RM and KM, this work was supported by the Australian Antarctic Division (AAD), the Australian Government's Australian Antarctic Program Partnership (AAPP), and the Australian Research Council Special Research Initiative the
755 Australian Centre for Excellence in Antarctic Science (Project Number SR200100008). LGB is funded by the Australian Research Council (FT190100404, DP240100325). PU is funded by the EU Horizon 2020 PolarRES project (grant number 101003590) and by the Research Council of Finland (grant number 364876). For DKP, this work was supported by US NA24OARX431G0018 and US NSF-OPP-2138785. BL gratefully acknowledges financial support from ONR (N00014-23-1-2484) and NSF (ARCSS 2138787 and Arctic Natural Sciences 2143547). AT acknowledges support from the Australian
760 Research Council (LE220100103, DP240100325). ADF is supported by the Australian Research Council (FT230100234, LP170101090, LE220100103 and DP240100325). PW's contribution is funded by AAPP, ACEAS and the Australian Research Council's Special Research Initiative for Antarctic Gateway Partnership (Project ID SR140300001). SC is funded by the AAD, AAPP and International Space Science Institute team grant #501.

14 References

- 765 Ackley, S. F.: Pressure ridge associated microbial communities in Antarctic sea ice, *Eos, Trans. Am. Geophys. Union*, 66, 1278, <https://doi.org/10.1029/EO066i051p01257>, 1985.
- Ackley, S. F. and Sullivan, C. W.: Physical controls on the development and characteristics of Antarctic sea ice biological communities - A review and synthesis, *Deep-Sea Res. Part I: Oceanographic Research Papers*, 41, 1583–1604, [https://doi.org/10.1016/0967-0637\(94\)90062-0](https://doi.org/10.1016/0967-0637(94)90062-0), 1994.
- 770 Ackley, S. F., Stammerjohn, S., Maksym, T., Smith, M., Cassano, J., Guest, P., Tison, J. L., Delille, B., Loose, B., Sedwick, P., DePace, L., Roach, L., and Parno, J.: Sea-ice production and air/ice/ocean/biogeochemistry interactions in the Ross Sea during the PIPERS 2017 autumn field campaign, *Ann. Glaciol.*, 61, 181–195, <https://doi.org/10.1017/aog.2020.31>, 2020.
- Alberello, A., Bennetts, L. G., Onorato, M., Vichi, M., MacHutchon, K., Eayrs, C., Ntamba, B. N., Benetazzo, A., Bergamasco,



- F., Nelli, F., Pattani, R., Clarke, H., Tersigni, I., and Toffoli, A.: Three-dimensional imaging of waves and floes in the marginal ice zone during a cyclone, *Nat. Commun.*, 13, 4590, <https://doi.org/10.1038/s41467-022-32036-2>, 2022.
- Allison, I., Brandt, R. E., and Warren, S. G.: East Antarctic sea ice: Albedo, thickness distribution, and snow cover, *J. Geophys. Res.: Oceans*, 98, 12417–12429, <https://doi.org/10.1029/93jc00648>, 1993.
- Andreas, E. L. and Ackley, S. F.: On the Differences in Ablation Seasons of Arctic and Antarctic Sea Ice, *J. Atmos. Sc.*, 39, 440–447, [https://doi.org/10.1175/1520-0469\(1982\)039<0440:Otdias>2.0.Co;2](https://doi.org/10.1175/1520-0469(1982)039<0440:Otdias>2.0.Co;2), 1982.
- 780 Arrigo, K. R., Brown, Z. W., Mills, M. M., Deming, J. W., and Tremblay, J.-É.: Sea ice algal biomass and physiology in the Amundsen Sea, Antarctica, *Elem. Sc. Anthropol.*, 2, <https://doi.org/10.12952/journal.elementa.000028>, 2014.
- Arrigo, K. R. and van Dijken, G. L.: Phytoplankton dynamics within 37 Antarctic coastal polynya systems, *J. Geophys. Res. Oceans*, 108, <https://doi.org/10.1029/2002jc001739>, 2003.
- Asplin, M. G., Galley, R., Barber, D. G., and Prinsenberg, S.: Fracture of summer perennial sea ice by ocean swell as a result of Arctic storms, *J. Geophys. Res. Oceans*, 117, <https://doi.org/10.1029/2011jc007221>, 2012.
- 785 Asplin, M. G., Scharien, R., Else, B., Howell, S., Barber, D. G., Papakyriakou, T., and Prinsenberg, S.: Implications of fractured Arctic perennial ice cover on thermodynamic and dynamic sea ice processes, *J. Geophys. Res. Oceans*, 119, 2327–2343, <https://doi.org/10.1002/2013jc009557>, 2014.
- Auger, M., Sallée, J. B., Thompson, A. F., Pauthenet, E., and Prandi, P.: Southern Ocean Ice-Covered Eddy Properties From Satellite Altimetry, *J. Geophys. Res. Oceans*, 128, <https://doi.org/10.1029/2022jc019363>, 2023.
- 790 Ayres, H. C., Screen, J. A., Blockley, E. W., and Bracegirdle, T. J.: The Coupled Atmosphere–Ocean Response to Antarctic Sea Ice Loss, *J. Clim.*, 35, 4665–4685, <https://doi.org/10.1175/jcli-d-21-0918.1>, 2022.
- Barber, D. G. and Massom, R. A.: The Role of Sea Ice in Arctic and Antarctic Polynyas, in: *Polynyas: Windows to the World*, edited by: Smith, W. O., and Barber, D. G., Elsevier Oceanography Series, 1–54, [https://doi.org/10.1016/s0422-9894\(06\)74001-6](https://doi.org/10.1016/s0422-9894(06)74001-6), 2007.
- 795 Bateson, A. W., Feltham, D. L., Schröder, D., Hosekova, L., Ridley, J. K., and Aksenov, Y.: Impact of sea ice floe size distribution on seasonal fragmentation and melt of Arctic sea ice, *The Cryosphere*, 14, 403–428, <https://doi.org/10.5194/tc-14-403-2020>, 2020.
- Bennetts, L. G., O'Farrell, S., and Uotila, P.: Brief communication: Impacts of ocean-wave-induced breakup of Antarctic sea ice via thermodynamics in a stand-alone version of the CICE sea-ice model, *The Cryosphere*, 11, 1035–1040, <https://doi.org/10.5194/tc-11-1035-2017>, 2017.
- 800 Bennetts, L. G., Shakespeare, C. J., Vreugdenhil, C. A., Foppert, A., Gayen, B., Meyer, A., Morrison, A. K., Padman, L., Phillips, H. E., Stevens, C. L., Toffoli, A., Constantinou, N. C., Cusack, J. M., Cyriac, A., Doddridge, E. W., England, M. H., Evans, D. G., Heil, P., Hogg, A. M., Holmes, R. M., Huneke, W. G. C., Jones, N. L., Keating, S. R., Kiss, A. E., Kraitzman, N., Malyarenko, A., McConnochie, C. D., Meucci, A., Montiel, F., Neme, J., Nikurashin, M., Patel, R. S., Peng, J. P., Rayson, M., Rosevear, M. G., Sohail, T., Spence, P., and Stanley, G. J.: Closing the Loops on Southern Ocean Dynamics: From the Circumpolar Current to Ice Shelves and From Bottom Mixing to Surface Waves, *Rev. Geophys.*, 62,



<https://doi.org/10.1029/2022rg000781>, 2024.

- Bennetts, L. G. and Williams, T. D.: Water wave transmission by an array of floating discs, *Proceedings of the Royal Society A: Mathematical, Physical and Engineering Sciences*, 471, <https://doi.org/10.1098/rspa.2014.0698>, 2015.
- Brandt, R. E., Warren, S. G., Worby, A. P., and Grenfell, T. C.: Surface Albedo of the Antarctic Sea Ice Zone, *J. Clim.*, 18, 3606–3622, <https://doi.org/10.1175/jcli3489.1>, 2005.
- Brouwer, J., Fraser, A. D., Murphy, D. J., Wongpan, P., Alberello, A., Kohout, A., Horvat, C., Wotherspoon, S., Massom, R. A., Cartwright, J., and Williams, G. D.: Altimetric observation of wave attenuation through the Antarctic marginal ice zone using ICESat-2, *The Cryosphere*, 16, 2325–2353, <https://doi.org/10.5194/tc-16-2325-2022>, 2022.
- Casas-Prat, M., Hemer, M. A., Dodet, G., Morim, J., Wang, X. L., Mori, N., Young, I., Erikson, L., Kamranzad, B., Kumar, P., Menéndez, M., and Feng, Y.: Wind-wave climate changes and their impacts, *Nature Reviews Earth & Environment*, 5, 23–42, <https://doi.org/10.1038/s43017-023-00502-0>, 2024.
- Cavalieri, D., Parkinson, C., Gloersen, P., and Zwally, H. J.: Sea ice concentrations from Nimbus-7 SMMR and DMSP SSM/I-SSMIS passive microwave data, NSIDC-0051 Version 1, Boulder, Colorado, USA, NASA National Snow and Ice Data Center Distributed Active Archive Center, <https://doi.org/10.5067/8GQ8LZQVL0VL>, 1996.
- Chai, W., Leira, B. J., Høyland, K. V., Sinsabvarodom, C., and Yu, Z.: Statistics of thickness and strength of first-year ice along the Northern Sea Route, *Journal of Marine Science and Technology*, 26, 331–343, <https://doi.org/10.1007/s00773-020-00742-5>, 2020.
- Charlson, R. J., Lovelock, J. E., Andreae, M. O., and Warren, S. G.: Oceanic phytoplankton, atmospheric sulphur, cloud albedo and climate, *Nature*, 326, 655–661, <https://doi.org/10.1038/326655a0>, 1987.
- Comiso, J. C., Gersten, R. A., Stock, L. V., Turner, J., Perez, G. J., and Cho, K.: Positive Trend in the Antarctic Sea Ice Cover and Associated Changes in Surface Temperature, *J. Clim.*, 30, 2251–2267, <https://doi.org/10.1175/jcli-d-16-0408.1>, 2017a.
- Comiso, J. C., Meier, W. N., and Gersten, R.: Variability and trends in the Arctic Sea ice cover: Results from different techniques, *J. Geophys. Res. Oceans*, 122, 6883–6900, <https://doi.org/10.1002/2017jc012768>, 2017b.
- Comiso, J. C. and Steffen, K.: Studies of Antarctic sea ice concentrations from satellite data and their applications, *J. Geophys. Res. Oceans*, 106, 31361–31385, <https://doi.org/10.1029/2001jc000823>, 2001.
- Comiso, J. C., Grenfell, T. C., Lange, M., Lohanick, A. W., Moore, R. K., and Wadhams, P.: Microwave remote sensing of the Southern Ocean ice cover, in: *Microwave Remote Sensing of Sea Ice*, edited by Carsey, F. D., *Geophysical Monograph Series*, American Geophysical Union, Washington DC, USA, 243–259, <https://doi.org/10.1029/GM068p0243>, 1992.
- Corkill, M., Moreau, S., Janssens, J., Fraser, A. D., Heil, P., Tison, J. L., Cougnon, E. A., Genovese, C., Kimura, N., Meiners, K. M., Wongpan, P., and Lannuzel, D.: Physical and Biogeochemical Properties of Rotten East Antarctic Summer Sea Ice, *J. Geophys. Res. Oceans*, 128, <https://doi.org/10.1029/2022jc018875>, 2023.
- Curry, J. A., Schramm, J. L., and Ebert, E. E.: Sea Ice-Albedo Climate Feedback Mechanism, *J. Clim.*, 8, 240–247, [https://doi.org/10.1175/1520-0442\(1995\)008<0240:Siacfm>2.0.Co;2](https://doi.org/10.1175/1520-0442(1995)008<0240:Siacfm>2.0.Co;2), 1995.
- Curry, J. A., Schramm, J. L., Perovich, D. K., and Pinto, J. O.: Applications of SHEBA/FIRE data to evaluation of snow/ice



- albedo parameterizations, *J. Geophys. Res. Atmos.*, 106, 15345–15355, <https://doi.org/10.1029/2000jd900311>, 2001.
- Dai, M., Shen, H. H., Hopkins, M. A., and Ackley, S. F.: Wave rafting and the equilibrium pancake ice cover thickness, *J. Geophys. Res. Oceans*, 109, <https://doi.org/10.1029/2003jc002192>, 2004.
- 845 Dalman, L. A., Meiners, K. M., Thomas, D. N., Deman, F., Bestley, S., Moreau, S., Arrigo, K. R., Campbell, K., Corkill, M., Cozzi, S., Delille, B., Fransson, A., Fraser, A. D., Henley, S. F., Janssens, J., Lannuzel, D., Munro, D. R., Nomura, D., Norman, L., Papadimitriou, S., Schallenberg, C., Tison, J. L., Vancoppenolle, M., van der Merwe, P., and Fripiat, F.: Observation-Based Estimate of Net Community Production in Antarctic Sea Ice, *Geophys. Res. Lett.*, 52, <https://doi.org/10.1029/2024gl113717>, 2025.
- 850 Day, N. S., Bennetts, L. G., O’Farrell, S. P., Alberello, A., and Montiel, F.: Analysis of the Antarctic Marginal Ice Zone Based on Unsupervised Classification of Standalone Sea Ice Model Data, *J. Geophys. Res. Oceans*, 129, <https://doi.org/10.1029/2024jc020953>, 2024.
- Drinkwater, M. R. and Xiang, L.: Seasonal to interannual variability in Antarctic sea-ice surface melt, *IEEE Trans. Geosc. Rem. Sens.*, 38, 1827–1842, <https://doi.org/10.1109/36.851767>, 2000.
- 855 Dubey, U., Willmes, S., and Heinemann, G.: A new dataset of Southern Ocean sea-ice leads: First insights into regional lead patterns, seasonality and trends, 2003–2023, *EGUsphere [preprint]*, doi: 10.5194/egusphere-2025-736, 2025. <https://doi.org/10.5194/egusphere-2025-736>, 2025.
- Ducklow, H., Fraser, W., Meredith, M., Stammerjohn, S., Doney, S., Martinson, D., Salliey, S., Schofield, O., Steinberg, D., Venables, H., and Amsler, C.: West Antarctic Peninsula: An Ice-Dependent Coastal Marine Ecosystem in Transition, *Oceanog.*, 26, 190–203, <https://doi.org/10.5670/oceanog.2013.62>, 2013.
- 860 Eayrs, C., Holland, D., Francis, D., Wagner, T., Kumar, R., and Li, X.: Understanding the Seasonal Cycle of Antarctic Sea Ice Extent in the Context of Longer-Term Variability, *Rev. Geophys.*, 57, 1037–1064, <https://doi.org/10.1029/2018rg000631>, 2019.
- Ebert, E. E. and Curry, J. A.: An intermediate one-dimensional thermodynamic sea ice model for investigating ice-atmosphere interactions, *J. Geophys. Res. Oceans*, 98, 10085–10109, <https://doi.org/10.1029/93jc00656>, 1993.
- 865 Eicken, H., Ackley, S. F., Richter-Menge, J. A., and Lange, M. A.: Is the strength of sea ice related to its chlorophyll content?, *Polar Biol.*, 11, <https://doi.org/10.1007/bf00239027>, 1991.
- Eicken, H., Fischer, H., and Lemke, P.: Effects of the snow cover on Antarctic sea ice and potential modulation of its response to climate change, *Ann. Glaciol.*, 21, 369–376, <https://doi.org/10.3189/s0260305500016086>, 1995.
- 870 Eicken, H., Lange, M. A., and Wadhams, P.: Characteristics and distribution patterns of snow and meteoric ice in the Weddell Sea and their contribution to the mass balance of sea ice, *Ann. Geophys.*, 12, 80–93, <https://doi.org/10.1007/s00585-994-0080-x>, 1994.
- England, M., Polvani, L., and Sun, L.: Contrasting the Antarctic and Arctic Atmospheric Responses to Projected Sea Ice Loss in the Late Twenty-First Century, *J. Clim.*, 31, 6353–6370, <https://doi.org/10.1175/jcli-d-17-0666.1>, 2018.
- 875 England, M. R., Polvani, L. M., Sun, L., and Deser, C.: Tropical climate responses to projected Arctic and Antarctic sea-ice



- loss, *Nat. Geosc.*, 13, 275–281, <https://doi.org/10.1038/s41561-020-0546-9>, 2020.
- Enomoto, H. and Ohmura, A.: The influences of atmospheric half-yearly cycle on the sea ice extent in the Antarctic, *J. Geophys. Res. Oceans*, 95, 9497–9511, <https://doi.org/10.1029/JC095iC06p09497>, 1990.
- Fang, Y., Wu, T., Hu, A., and Chu, M.: A modified thermodynamic sea ice model and its application, *Oc. Modell.*, 178,
880 <https://doi.org/10.1016/j.ocemod.2022.102096>, 2022.
- Fetterer, F. and Untersteiner, N.: Observations of melt ponds on Arctic sea ice, *J. Geophys. Res. Oceans*, 103, 24821–24835, <https://doi.org/10.1029/98jc02034>, 1998.
- Fitzpatrick, M. F. and Warren, S. G.: Transmission of Solar Radiation by Clouds over Snow and Ice Surfaces. Part II: Cloud Optical Depth and Shortwave Radiative Forcing from Pyranometer Measurements in the Southern Ocean, *J. Clim.*, 18, 4637–
885 4648, <https://doi.org/10.1175/jcli3562.1>, 2005.
- Fitzpatrick, M. F. and Warren, S. G.: The Relative Importance of Clouds and Sea Ice for the Solar Energy Budget of the Southern Ocean, *J. Clim.*, 20, 941–954, <https://doi.org/10.1175/jcli4040.1>, 2007.
- Flocco, D., Feltham, D. L., and Turner, A. K.: Incorporation of a physically based melt pond scheme into the sea ice component of a climate model, *J. Geophys. Res. Oceans*, 115, <https://doi.org/10.1029/2009jc005568>, 2010.
- 890 Fraser, A. D., et al.: Revealing the Antarctic marginal ice zone: a decade-long wave-in-ice climatology, submitted.
- Frölicher, T. L., Sarmiento, J. L., Paynter, D. J., Dunne, J. P., Krasting, J. P., and Winton, M.: Dominance of the Southern Ocean in Anthropogenic Carbon and Heat Uptake in CMIP5 Models, *J. Clim.*, 28, 862–886, <https://doi.org/10.1175/jcli-d-14-00117.1>, 2015.
- Garrison, D. L., Jeffries, M. O., Gibson, A., Coale, S. L., Neenan, D., Fritsen, C., Okolodkov, Y. B., and Gowing, M. M.:
895 Development of sea ice microbial communities during autumn ice formation in the Ross Sea, *Mar. Ecol. Prog. Ser.*, 259, 1–15, <https://doi.org/10.3354/meps259001>, 2003.
- Godfred-Spenning, C. R., and Simmonds, I.: An Analysis of Antarctic Sea-Ice and Extratropical Cyclone Associations, *Int. J. Climatol.*, 16, 1315–1332, [https://doi.org/10.1002/\(sici\)1097-0088\(199612\)16:12<1315::Aid-joc92>3.0.Co;2-m](https://doi.org/10.1002/(sici)1097-0088(199612)16:12<1315::Aid-joc92>3.0.Co;2-m), 1996.
- Golden, K. M., Ackley, S. F., and Lytle, V. I.: The Percolation Phase Transition in Sea Ice, *Science*, 282, 2238–2241,
900 <https://www.science.org/doi/10.1126/science.282.5397.2238>, 1998.
- Goosse, H., Allende Contador, S., Bitz, C. M., Blanchard-Wrigglesworth, E., Eayrs, C., Fichefet, T., Himmich, K., Huot, P.-V., Klein, F., Marchi, S., Massonnet, F., Mezzina, B., Pelletier, C., Roach, L., Vancoppenolle, M., and van Lipzig, N. P. M.: Modulation of the seasonal cycle of the Antarctic sea ice extent by sea ice processes and feedbacks with the ocean and the atmosphere, *The Cryosphere*, 17, 407–425, <https://doi.org/10.5194/tc-17-407-2023>, 2023.
- 905 Goosse, H., Kay, J. E., Armour, K. C., Bodas-Salcedo, A., Chepfer, H., Docquier, D., Jonko, A., Kushner, P. J., Lecomte, O., Massonnet, F., Park, H. S., Pithan, F., Svensson, G., and Vancoppenolle, M.: Quantifying climate feedbacks in polar regions, *Nat. Commun.*, 9, 1919, <https://doi.org/10.1038/s41467-018-04173-0>, 2018.
- Gordon, A. L.: Seasonality of Southern Ocean sea ice, *J. Geophys. Res. Oceans*, 86, 4193–4197, <https://doi.org/10.1029/JC086iC05p04193>, 1981.



- 910 Gordon, A. L. and Taylor, H. W.: Seasonal change of Antarctic sea ice cover, *Science*, 187, 346–347, <https://doi.org/10.1126/science.187.4174.346>, 1975.
- Grenfell, T. C. and Maykut, G. A.: The Optical Properties of Ice and Snow in the Arctic Basin, *J. Glac.*, 18, 445–463, <https://doi.org/10.3189/s0022143000021122>, 1977.
- Grenfell, T. C. and Perovich, D. K.: Seasonal and spatial evolution of albedo in a snow-ice-land-ocean environment, *J. Geophys. Res. Oceans*, 109, <https://doi.org/10.1029/2003jc001866>, 2004.
- 915 Hague, M. and Vichi, M.: Southern Ocean Biogeochemical Argo detect under-ice phytoplankton growth before sea ice retreat, *Biogeosc.*, 18, 25–38, <https://doi.org/10.5194/bg-18-25-2021>, 2021.
- Hartmann, D. L.: *Global Physical Climatology (Second Edition)*, Elsevier, Boston, 978-0-12-328531-7, 2016.
- Haumann, F. A., Gruber, N., Munnich, M., Frenger, I., and Kern, S.: Sea-ice transport driving Southern Ocean salinity and its recent trends, *Nature*, 537, 89–92, <https://doi.org/10.1038/nature19101>, 2016.
- 920 Herman, A. and Bradtke, K.: Fetch-Limited, Strongly Forced Wind Waves in Waters With Frazil and Grease Ice – Spectral Modeling and Satellite Observations in an Antarctic Coastal Polynya, *J. Geophys. Res. Oceans*, 129, <https://doi.org/10.1029/2023jc020452>, 2024.
- Hobbs, W., Spence, P., Meyer, A., Schroeter, S., Fraser, A. D., Reid, P., Tian, T. R., Wang, Z., Liniger, G., Doddridge, E. W., and Boyd, P. W.: Observational Evidence for a Regime Shift in Summer Antarctic Sea Ice, *J. Clim.*, 37, 2263–2275, <https://doi.org/10.1175/jcli-d-23-0479.1>, 2024.
- 925 Holland, M. M. and Bitz, C. M.: Polar amplification of climate change in coupled models, *Clim. Dyn.*, 21, 221–232, <https://doi.org/10.1007/s00382-003-0332-6>, 2003.
- Horvat, C.: Floes, the marginal ice zone and coupled wave-sea-ice feedbacks, *Phil. Trans. A. Math. Phys. Eng. Sci.*, 380, 20210252, <https://doi.org/10.1098/rsta.2021.0252>, 2022.
- 930 Horvat, C. and Tziperman, E.: Understanding Melting due to Ocean Eddy Heat Fluxes at the Edge of Sea-Ice Floes, *Geophys. Res. Lett.*, 45, 9721–9730, <https://doi.org/10.1029/2018gl079363>, 2018.
- Horvat, C., Bisson, K., Seabrook, S., Cristi, A. and Matthes, L. C.: Evidence of phytoplankton blooms under Antarctic sea ice, *Front. Mar. Sci.* 9:942799. doi: 10.3389/fmars.2022.942799, 2022.
- 935 Inoue, J., Kikuchi, T., and Perovich, D. K.: Effect of heat transmission through melt ponds and ice on melting during summer in the Arctic Ocean, *J. Geophys. Res. Oceans*, 113, <https://doi.org/10.1029/2007jc004182>, 2008.
- IPCC (Intergovernmental Panel on Climate Change): Observations: Atmosphere and Surface, in: *Climate Change 2013 – The Physical Science Basis: Working Group I Contribution to the Fifth Assessment Report of the Intergovernmental Panel on Climate Change*, 159–254, Cambridge University Press, 2014.
- 940 Ishida, K. and Ohshima, K. I.: Ice-band characteristics of the Antarctic seasonal ice zone observed using MOS MESSR images, *Atmos.-Ocean*, 47, 169–183, <https://doi.org/10.3137/oc300.2009>, 2009.
- Ivanova, N., Pedersen, L. T., Tonboe, R. T., Kern, S., Heygster, G., Lavergne, T., Sørensen, A., Saldo, R., Dybkjær, G., Brucker, L., and Shokr, M.: Inter-comparison and evaluation of sea ice algorithms: towards further identification of challenges



- and optimal approach using passive microwave observations, *The Cryosphere*, 9, 1797–1817, <https://doi.org/10.5194/tc-9-1797-2015>, 2015.
- Kacimi, S. and Kwok, R.: The Antarctic sea ice cover from ICESat-2 and CryoSat-2: freeboard, snow depth, and ice thickness, *The Cryosphere*, 14, 4453–4474, <https://doi.org/10.5194/tc-14-4453-2020>, 2020.
- Kashiwase, H., Ohshima, K. I., Nihashi, S., and Eicken, H.: Evidence for ice-ocean albedo feedback in the Arctic Ocean shifting to a seasonal ice zone, *Sci. Rep.*, 7, 8170, <https://doi.org/10.1038/s41598-017-08467-z>, 2017.
- 950 Kennicutt, M. C., Chown, S. L., Cassano, J. J., Liggett, D., Peck, L. S., Massom, R., Rintoul, S. R., Storey, J., Vaughan, D. G., Wilson, T. J., Allison, I., Ayton, J., Badhe, R., Baeseman, J., Barrett, P. J., Bell, R. E., Bertler, N., Bo, S., Brandt, A., Bromwich, D., Cary, S. C., Clark, M. S., Convey, P., Costa, E. S., Cowan, D., Deconto, R., Dunbar, R., Elfring, C., Escutia, C., Francis, J., Fricker, H. A., Fukuchi, M., Gilbert, N., Gutt, J., Havermans, C., Hik, D., Hosie, G., Jones, C., Kim, Y. D., Le Maho, Y., Lee, S. H., Leppe, M., Leitchenkov, G., Li, X., Lipenkov, V., Lochte, K., López-Martínez, J., Lüdecke, C., Lyons, W., Marensi, S., Miller, H., Morozova, P., Naish, T., Nayak, S., Ravindra, R., Retamales, J., Ricci, C. A., Rogan-Finnemore, M., Ropert-Coudert, Y., Samah, A. A., Sanson, L., Scambos, T., Schloss, I. R., Shiraishi, K., Siegert, M. J., Simões, J. C., Storey, B., Sparrow, M. D., Wall, D. H., Walsh, J. C., Wilson, G., Winther, J. G., Xavier, J. C., Yang, H., and Sutherland, W. J.: A roadmap for Antarctic and Southern Ocean science for the next two decades and beyond, *Ant. Sc.*, 27, 3–18, <https://doi.org/10.1017/s0954102014000674>, 2014.
- 960 Kimura, N., Onomura, T., and Kikuchi, T.: Processes governing seasonal and interannual change of the Antarctic sea-ice area, *J. Oceanogr.*, 79, 109–121, <https://doi.org/10.1007/s10872-022-00669-y>, 2022.
- Kohout, A. L., Williams, M. J., Dean, S. M., and Meylan, M. H.: Storm-induced sea-ice breakup and the implications for ice extent, *Nature*, 509, 604–607, <https://doi.org/10.1038/nature13262>, 2014.
- Kohout, A. L., Williams, M. J. M., Toyota, T., Lieser, J., and Hutchings, J.: In situ observations of wave-induced sea ice breakup, *Deep-Sea Res. Part B: Top. St. Oceanogr.*, 131, 22–27, <https://doi.org/10.1016/j.dsr2.2015.06.010>, 2016.
- Kottmeier, S. T. and Sullivan, C. W.: Bacterial biomass and production in pack ice of Antarctic marginal ice edge zones, *Deep-Sea Res. Part A. Oceanogr. Res. Papers*, 37, 1311–1330, [https://doi.org/10.1016/0198-0149\(90\)90045-w](https://doi.org/10.1016/0198-0149(90)90045-w), 1990.
- Light, B., Perovich, D. K., Webster, M. A., Polashenski, C., and Dadic, R.: Optical properties of melting first-year Arctic sea ice, *J. Geophys. Res. Oceans*, 120, 7657–7675, <https://doi.org/10.1002/2015jc011163>, 2015.
- 970 Light, B., Smith, M. M., Perovich, D. K., Webster, M. A., Holland, M. M., Linhardt, F., Raphael, I. A., Clemens-Sewall, D., Macfarlane, A. R., Anhaus, P., and Bailey, D. A.: Arctic sea ice albedo: Spectral composition, spatial heterogeneity, and temporal evolution observed during the MOSAiC drift, *Elem.: Sc. Anthropol.*, 10, <https://doi.org/10.1525/elementa.2021.000103>, 2022.
- Liu, A. K. and Mollo-Christensen, E.: Wave Propagation in a Solid Ice Pack, *J. Phys. Oceanogr.*, 18, 1702–1712, [https://doi.org/10.1175/1520-0485\(1988\)018<1702:Wpiasi>2.0.Co;2](https://doi.org/10.1175/1520-0485(1988)018<1702:Wpiasi>2.0.Co;2), 1988.
- Louw, S. D. V., Walker, D. R., and Fawcett, S. E.: Factors influencing sea-ice algae abundance, community composition, and distribution in the marginal ice zone of the Southern Ocean during winter, *Deep-Sea Res. Part A. Oceanogr. Res. Papers*, 185,



- <https://doi.org/10.1016/j.dsr.2022.103805>, 2022.
- Lüthje, M., Feltham, D. L., Taylor, P. D., and Worster, M. G.: Modeling the summertime evolution of sea-ice melt ponds, *J. Geophys. Res. Oceans*, 111, <https://doi.org/10.1029/2004jc002818>, 2006.
- Maksym, T.: Arctic and Antarctic Sea Ice Change: Contrasts, Commonalities, and Causes, *Ann. Rev. Mar. Sci.*, 11, 187–213, <https://doi.org/10.1146/annurev-marine-010816-060610>, 2019.
- Maksym, T. and Markus, T.: Antarctic sea ice thickness and snow-to-ice conversion from atmospheric reanalysis and passive microwave snow depth, *J. Geophys. Res. Oceans*, 113, <https://doi.org/10.1029/2006jc004085>, 2008.
- 985 Maksym, T., Stammerjohn, S., Ackley, S., and Massom, R.: Antarctic Sea Ice—A Polar Opposite?, *Oceanogr.*, 25, 140–151, <https://doi.org/10.5670/oceanog.2012.88>, 2012.
- Manabe, S. and Stouffer, R. J.: Sensitivity of a global climate model to an increase of CO₂ concentration in the atmosphere, *J. Geophys. Res. Oceans*, 85, 5529–5554, <https://doi.org/10.1029/JC085iC10p05529>, 1980.
- Martin, S., Kauffman, P., and Parkinson, C.: The movement and decay of ice edge bands in the winter Bering Sea, *J. Geophys. Res. Oceans*, 88, 2803–2812, <https://doi.org/10.1029/JC088iC05p02803>, 1983.
- 990 Maslanik, J. A., Fowler, C., Stroeve, J., Drobot, S., Zwally, J., Yi, D., and Emery, W.: A younger, thinner Arctic ice cover: Increased potential for rapid, extensive sea-ice loss, *Geophys. Res. Lett.*, 34, <https://doi.org/10.1029/2007gl032043>, 2007.
- Massom, R. A.: *Satellite Remote Sensing of Polar Regions: Applications, Limitations and Data Availability*, Belhaven Press, London (UK) and Lewis Publishers, Boca Raton (USA), 307 pp., ISBN 0-87372-607-8, 1991.
- 995 Massom, R. A. and Stammerjohn, S. E.: Antarctic sea ice change and variability – Physical and ecological implications, *Polar Sc.*, 4, 149–186, <https://doi.org/10.1016/j.polar.2010.05.001>, 2010.
- Massom, R. A., Drinkwater, M. R., and Haas, C.: Winter snow cover on sea ice in the Weddell Sea, *J. Geophys. Res. Oceans*, 102, 1101–1117, <https://doi.org/10.1029/96jc02992>, 1997.
- Massom, R. A., Lytle, V. I., Worby, A. P., and Allison, I.: Winter snow cover variability on East Antarctic sea ice, *J. Geophys. Res. Oceans*, 103, 24837–24855, <https://doi.org/10.1029/98jc01617>, 1998.
- 1000 Massom, R. A., Comiso, J. C., Worby, A. P., Lytle, V. I., and Stock, L.: Regional Classes of Sea Ice Cover in the East Antarctic Pack Observed from Satellite and In Situ Data during a Winter Time Period, *Remote Sensing of Environment*, 68, 61–76, [https://doi.org/10.1016/s0034-4257\(98\)00100-x](https://doi.org/10.1016/s0034-4257(98)00100-x), 1999.
- Massom, R. A., Eicken, H., Hass, C., Jeffries, M. O., Drinkwater, M. R., Sturm, M., Worby, A. P., Wu, X., Lytle, V. I., Ushio, S., Morris, K., Reid, P. A., Warren, S. G., and Allison, I.: Snow on Antarctic sea ice, *Rev. Geophys.*, 39, 413–445, <https://doi.org/10.1029/2000rg000085>, 2001.
- Massom, R. A., Jacka, K., Pook, M. J., Fowler, C., Adams, N., and Bindoff, N.: An anomalous late-season change in the regional sea ice regime in the vicinity of the Mertz Glacier Polynya, East Antarctica, *J. Geophys. Res. Oceans*, 108, <https://doi.org/10.1029/2002jc001354>, 2003.
- 1010 Massom, R. A., Stammerjohn, S. E., Smith, R. C., Pook, M. J., Iannuzzi, R. A., Adams, N., Martinson, D. G., Vernet, M., Fraser, W. R., Quetin, L. B., Ross, R. M., Massom, Y., and Krouse, H. R.: Extreme Anomalous Atmospheric Circulation in



the West Antarctic Peninsula Region in Austral Spring and Summer 2001/02, and Its Profound Impact on Sea Ice and Biota, *J. Clim.*, 19, 3544–3571, <https://doi.org/10.1175/jcli3805.1>, 2006.

Massom, R. A., Stammerjohn, S. E., Lefebvre, W., Harangozo, S. A., Adams, N., Scambos, T. A., Pook, M. J., and Fowler, C.: West Antarctic Peninsula sea ice in 2005: Extreme ice compaction and ice edge retreat due to strong anomaly with respect to climate, *J. Geophys. Res. Oceans*, 113, <https://doi.org/10.1029/2007jc004239>, 2008.

Massom, R. A., Reid, P., Stammerjohn, S., Raymond, B., Fraser, A., and Ushio, S.: Change and variability in East Antarctic sea ice seasonality, 1979/80–2009/10, *PLoS One*, 8, e64756, <https://doi.org/10.1371/journal.pone.0064756>, 2013.

Massom, R. A., Scambos, T. A., Bennetts, L. G., Reid, P., Squire, V. A., and Stammerjohn, S. E.: Antarctic ice shelf disintegration triggered by sea ice loss and ocean swell, *Nature*, 558, 383–389, <https://doi.org/10.1038/s41586-018-0212-1>, 2018.

Maykut, G. A. and Perovich, D. K.: The role of shortwave radiation in the summer decay of a sea ice cover, *J. Geophys. Res. Oceans*, 92, 7032–7044, <https://doi.org/10.1029/JC092iC07p07032>, 1987.

Meehl, G. A. and Washington, W. M.: CO₂ climate sensitivity and snow-sea-ice albedo parameterization in an atmospheric GCM coupled to a mixed-layer ocean model, *Clim. Ch.*, 16, 283–306, <https://doi.org/10.1007/bf00144505>, 1990.

Mellor, M.: Mechanical Behavior of Sea Ice, in: *The Geophysics of Sea Ice*, edited by: Untersteiner, N., Springer, Boston, USA, 165–281, https://doi.org/10.1007/978-1-4899-5352-0_3, 1986.

Meredith, M., Sommerkorn, M., Cassotta, S., Derksen, C., Ekaykin, A., Hollowed, A., Kofinas, G., Mackintosh, A., Melbourne-Thomas, J., Muelbert, M. M. C., Ottersen, G., Pritchard, H., and Schuur, E. A. G.: Polar Regions. In: *The Ocean and Cryosphere in a Changing Climate*, Cambridge University Press, Cambridge UK., 203–320, <https://doi.org/10.1017/9781009157964.005>, 2022.

Meredith, M. P. and Brandon, M. A.: Oceanography and sea ice in the Southern Ocean, in: *Sea Ice*, edited by: Thomas, D. N., Wiley-Blackwell, Oxford (UK), 216–238, <https://doi.org/10.1002/9781118778371.ch8>, 2017.

Morim, J., Hemer, M., Wang, X. L., Cartwright, N., Trenham, C., Semedo, A., Young, I., Brichenno, L., Camus, P., Casas-Prat, M., Erikson, L., Mentaschi, L., Mori, N., Shimura, T., Timmermans, B., Aarnes, O., Breivik, Ø., Behrens, A., Dobrynin, M., Menendez, M., Staneva, J., Wehner, M., Wolf, J., Kamranzad, B., Webb, A., Stopa, J., and Andutta, F.: Robustness and uncertainties in global multivariate wind-wave climate projections, *Nat. Clim. Ch.*, 9, 711–718, <https://doi.org/10.1038/s41558-019-0542-5>, 2019.

Morris, K., Jeffries, M., and Li, S.: Sea Ice Characteristics and Seasonal Variability of ERS-1 SAR Backscatter in the Bellingshausen Sea, in *Antarctic Sea Ice Physical Processes, Interactions and Variability*, edited by: Jeffries, M. O., American Geophysical Union, Washington DC, USA, 213–242, <https://doi.org/10.1029/AR074>, 1998.

Muchow, M., Schmitt, A. U., and Kaleschke, L.: A lead-width distribution for Antarctic sea ice: a case study for the Weddell Sea with high-resolution Sentinel-2 images, *The Cryosphere*, 15, 4527–4537, <https://doi.org/10.5194/tc-15-4527-2021>, 2021. National Academies of Sciences, Engineering, and Medicine. 2017. *Antarctic Sea Ice Variability in the Southern Ocean-Climate System: Proceedings of a Workshop*, The National Academies Press, Washington DC, USA,



<https://doi.org/10.17226/24696>, 2017.

Nelli, F., Bennetts, Luke G., Skene, David M., and Toffoli, A.: Water wave transmission and energy dissipation by a floating plate in the presence of overwash, *J. Fluid Mech.*, 889, <https://doi.org/10.1017/jfm.2020.75>, 2020.

1050 Nicolaus, M., Gerland, S., Hudson, S. R., Hanson, S., Haapala, J., and Perovich, D. K.: Seasonality of spectral albedo and transmittance as observed in the Arctic Transpolar Drift in 2007, *J. Geophys. Res. Oceans*, 115, <https://doi.org/10.1029/2009jc006074>, 2010.

Nicolaus, M., Katlein, C., Maslanik, J., and Hendricks, S.: Changes in Arctic sea ice result in increasing light transmittance and absorption, *Geophys. Res. Lett.*, 39, <https://doi.org/10.1029/2012gl053738>, 2012.

1055 Nihashi, S. and Cavalieri, D. J.: Observational evidence of a hemispheric-wide ice–ocean albedo feedback effect on Antarctic sea-ice decay, *J. Geophys. Res. Oceans*, 111, <https://doi.org/10.1029/2005jc003447>, 2006.

Nihashi, S. and Ohshima, K. I.: Relationship between ice decay and solar heating through open water in the Antarctic sea ice zone, *J. Geophys. Res. Oceans*, 106, 16767–16782, <https://doi.org/10.1029/2000jc000399>, 2001.

Nissen, C., Lovenduski, N. S., Brooks, C. M., Hoppema, M., Timmermann, R., and Hauck, J.: Severe 21st-century ocean acidification in Antarctic Marine Protected Areas, *Nat. Comm.*, 15, 259, <https://doi.org/10.1038/s41467-023-44438-x>, 2024.

1060 Nose, T., Katsuno, T., Waseda, T., Ushio, S., Rabault, J., Kodaira, T., and Voermans, J.: Observation of wave propagation over 1,000 km into Antarctica winter pack ice, *Coastal Eng. J.*, 66, 115–131, <https://doi.org/10.1080/21664250.2023.2283243>, 2023.

Notz, D. and Bitz, C. M.: Sea ice in Earth system models. In: *Sea Ice*, edited by: Thomas, D. N., Wiley-Blackwell, Oxford, UK, 304–325, <https://doi.org/https://doi.org/10.1002/9781118778371.ch12>, 2017.

1065 Ohshima, K. I. and Nihashi, S.: A Simplified Ice–Ocean Coupled Model for the Antarctic Ice Melt Season, *J. Phys. Oceanogr.*, 35, 188–201, <https://doi.org/10.1175/jpo-2675.1>, 2005.

Parkinson, C. L.: Global Sea Ice Coverage from Satellite Data: Annual Cycle and 35-Yr Trends, *J. Clim.*, 27, 9377–9382, <https://doi.org/10.1175/jcli-d-14-00605.1>, 2014.

1070 Parkinson, C. L.: A 40-y record reveals gradual Antarctic sea ice increases followed by decreases at rates far exceeding the rates seen in the Arctic, *Proc. Nat. Ac. Sci.*, 116, 14414–14423, <https://doi.org/10.1073/pnas.1906556116>, 2019.

Passerotti, G., Bennetts, L. G., von Bock und Polach, F., Alberello, A., Puolakka, O., Dolatshah, A., Monbaliu, J., and Toffoli, A.: Interactions between Irregular Wave Fields and Sea Ice: A Physical Model for Wave Attenuation and Ice Breakup in an Ice Tank, *J. Phys. Oceanogr.*, 52, 1431–1446, <https://doi.org/10.1175/jpo-d-21-0238.1>, 2022.

1075 Perovich, D. K.: The optical properties of sea ice, *CRREL Monograph 96-1*, US Army Corps of Engineers, Cold Regions Research and Engineering Laboratory, Hanover, USA, 25 pp., 1996.

Perovich, D. K.: On the aggregate-scale partitioning of solar radiation in Arctic sea ice during the Surface Heat Budget of the Arctic Ocean (SHEBA) field experiment, *J. Geophys. Res. Oceans*, 110, <https://doi.org/10.1029/2004jc002512>, 2005.

Perovich, D. K. and Richter-Menge, J. A.: Loss of sea ice in the Arctic, *Ann. Rev. Mar. Sc.*, 1, 417–441, <https://doi.org/10.1146/annurev.marine.010908.163805>, 2009.



- 1080 Perovich, D. K. and Jones, K. F.: The seasonal evolution of sea ice floe size distribution, *J. Geophys. Res. Oceans*, 119, 8767–8777, <https://doi.org/10.1002/2014jc010136>, 2014.
- Perovich, D. K., Grenfell, T. C., Richter-Menge, J. A., Light, B., Tucker, W. B., and Eicken, H.: Thin and thinner: Sea ice mass balance measurements during SHEBA, *J. Geophys. Res. Oceans*, 108, <https://doi.org/10.1029/2001jc001079>, 2003.
- Perovich, D. K., Richter-Menge, J. A., Jones, K. F., and Light, B.: Sunlight, water, and ice: Extreme Arctic sea ice melt during the summer of 2007, *Geophys. Res. Lett.*, 35, <https://doi.org/10.1029/2008gl034007>, 2008.
- 1085 Perovich, D. K., Grenfell, T. C., Light, B., Elder, B. C., Harbeck, J., Polashenski, C., Tucker, W. B., and Stelmach, C.: Transpolar observations of the morphological properties of Arctic sea ice, *J. Geophys. Res. Oceans*, 114, <https://doi.org/10.1029/2008jc004892>, 2009.
- Petrich, C., Eicken, H., Polashenski, C. M., Sturm, M., Harbeck, J. P., Perovich, D. K., and Finnegan, D. C.: Snow dunes: A controlling factor of melt pond distribution on Arctic sea ice, *J. Geophys. Res. Oceans*, 117, <https://doi.org/10.1029/2012jc008192>, 2012.
- 1090 Pitt, J. P. A., Bennetts, L. G., Meylan, M. H., Massom, R. A., and Toffoli, A.: Model Predictions of Wave Overwash Extent Into the Marginal Ice Zone, *J. Geophys. Res. Oceans*, 127, <https://doi.org/10.1029/2022jc018707>, 2022.
- Reid, P. and Massom, R.: Successive Antarctic sea ice extent records during 2012, 2013, and 2014, *Bull. Am. Met. Soc.*, 96, 7, S163–S164, 2015.
- 1095 Reid, P., Stammerjohn, S., Massom, R. A., Barreira, S., Scambos, T., and Lieser, J. L.: Sea-ice extent, concentration, and seasonality. In: *State of the Climate in 2023*, 8, *Bull. Am. Met. Soc.*, S331–S370, <https://doi.org/10.1175/bams-d-24-0099.1>, 2024.
- Reid, P., Stammerjohn, S., Massom, R. A., Barreira, S., Scambos, T., and Lieser, J. L.: Sea-ice extent, concentration, and seasonality. In: *State of the Climate in 2024*, *Bull. Amer. Meteor. Soc.*, In press.
- 1100 Riihelä, A., Bright, R. M., and Anttila, K.: Recent strengthening of snow and ice albedo feedback driven by Antarctic sea-ice loss, *Nat. Geosc.*, 14, 832–836, <https://doi.org/10.1038/s41561-021-00841-x>, 2021.
- Roach, L. A., Bitz, C. M., Horvat, C., and Dean, S. M.: Advances in Modeling Interactions Between Sea Ice and Ocean Surface Waves, *J. Adv. Model. Earth Syst.*, 11, 4167–4181, <https://doi.org/10.1029/2019ms001836>, 2019.
- 1105 Roach, L. A., Dörr, J., Holmes, C. R., Massonnet, F., Blockley, E. W., Notz, D., Rackow, T., Raphael, M. N., O'Farrell, S. P., Bailey, D. A., and Bitz, C. M.: Antarctic Sea Ice Area in CMIP6, *Geophys. Res. Lett.*, 47, <https://doi.org/10.1029/2019gl086729>, 2020.
- Roach, L. A., Eisenman, I., Wagner, T. J. W., Blanchard-Wrigglesworth, E., and Bitz, C. M.: Asymmetry in the seasonal cycle of Antarctic sea ice driven by insolation, *Nat. Geosc.*, 15, 277–281, <https://doi.org/10.1038/s41561-022-00913-6>, 2022.
- 1110 Saenz, B. T. and Arrigo, K. R.: Annual primary production in Antarctic sea ice during 2005–2006 from a sea ice state estimate, *J. Geophys. Res. Oceans*, 119, 3645–3678, <https://doi.org/10.1002/2013jc009677>, 2014.
- Saiki, R. and Mitsudera, H.: A Mechanism of Ice-Band Pattern Formation Caused by Resonant Interaction between Sea Ice and Internal Waves: A Theory, *J. Phys. Oceanogr.*, 46, 583–600, <https://doi.org/10.1175/jpo-d-14-0162.1>, 2016.



- Saiki, R., Mitsudera, H., Fujisaki-Manome, A., Kimura, N., Ukita, J., Toyota, T., and Nakamura, T.: Mechanism of ice-band pattern formation caused by resonant interaction between sea ice and internal waves in a continuously stratified ocean, *Progr. Oceanogr.*, 190, <https://doi.org/10.1016/j.pocean.2020.102474>, 2021.
- Screen, J. A. and Simmonds, I.: The central role of diminishing sea ice in recent Arctic temperature amplification, *Nature*, 464, 1334–1337, <https://doi.org/10.1038/nature09051>, 2010.
- Simmonds, I., Keay, K., and Lim, E.-P.: Synoptic Activity in the Seas around Antarctica, *Mon. Weath. Rev.*, 131, 272–288, [https://doi.org/10.1175/1520-0493\(2003\)131<0272:Saitsa>2.0.Co;2](https://doi.org/10.1175/1520-0493(2003)131<0272:Saitsa>2.0.Co;2), 2003.
- Skene, D. M., Bennetts, L. G., Meylan, M. H., and Toffoli, A.: Modelling water wave overwash of a thin floating plate, *J. Fluid Mech.*, 777, <https://doi.org/10.1017/jfm.2015.378>, 2015.
- Smith, D. M., Dunstone, N. J., Scaife, A. A., Fiedler, E. K., Copsey, D., and Hardiman, S. C.: Atmospheric Response to Arctic and Antarctic Sea Ice: The Importance of Ocean–Atmosphere Coupling and the Background State, *J. Clim.*, 30, 4547–4565, <https://doi.org/10.1175/jcli-d-16-0564.1>, 2017.
- Squire, V. A.: Of ocean waves and sea-ice revisited, *Cold Regions Science and Technology*, 49, 110–133, <https://doi.org/10.1016/j.coldregions.2007.04.007>, 2007.
- Squire, V. A.: Ocean Wave Interactions with Sea Ice: A Reappraisal, *Ann. Rev. Fluid Mech.*, 52, 37–60, <https://doi.org/10.1146/annurev-fluid-010719-060301>, 2020.
- Stammerjohn, S., Massom, R., Rind, D., and Martinson, D.: Regions of rapid sea ice change: An inter-hemispheric seasonal comparison, *Geophys. Res. Lett.*, 39, <https://doi.org/10.1029/2012gl050874>, 2012.
- Steele, M.: Sea ice melting and floe geometry in a simple ice-ocean model, *J. Geophys. Res. Oceans*, 97, 17729–17738, <https://doi.org/10.1029/92jc01755>, 2012.
- Stopa, J. E., Sutherland, P., and Arduin, F.: Strong and highly variable push of ocean waves on Southern Ocean sea ice, *Proc. Nat. Ac. Sc.*, 115, 5861–5865, <https://doi.org/10.1073/pnas.1802011115>, 2018.
- Sturm, M., and Massom, R. A.: Snow in the sea ice system: Friend or foe? In: *Sea Ice*, edited by: Thomas, D. N., Wiley-Blackwell, Oxford, UK, 65–109, <https://doi.org/10.1002/9781118778371.ch3>, 2017.
- Sutherland, P., and Dumont, D.: Marginal Ice Zone Thickness and Extent due to Wave Radiation Stress. *J. Phys. Oceanogr.*, 48, 1885–1901, <https://doi.org/10.1175/JPO-D-17-0167.1>, 2018.
- Takahashi, Y.: On the puddles of Lützow-Holm Bay, *Ant. Meteorol.*, Pergamon Press, New York, 321–332, 1960.
- Taylor, P. D. and Feltham, D. L.: A model of melt pond evolution on sea ice, *J. Geophys. Res. Oceans*, 109, <https://doi.org/10.1029/2004jc002361>, 2004.
- Teder, N. J., Bennetts, L. G., Reid, P. A., Massom, R. A., Pitt, J. P. A., Scambos, T. A., and Fraser, A. D.: Large-scale ice shelf calving events follow prolonged amplifications in flexure, *Nat. Geosc.*, in press.
- Thomson, J. and Rogers, W. E.: Swell and sea in the emerging Arctic Ocean, *Geophys. Res. Lett.*, 41, 3136–3140, <https://doi.org/10.1002/2014gl059983>, 2014.
- Timco, G. W. and Weeks, W. F.: A review of the engineering properties of sea ice, *Cold Regions Science and Technology*,



- 60, 107–129, <https://doi.org/10.1016/j.coldregions.2009.10.003>, 2010.
- Tison, J. L., Schwegmann, S., Dieckmann, G., Rintala, J. M., Meyer, H., Moreau, S., Vancoppenolle, M., Nomura, D., Engberg, S., Blomster, L. J., Hendricks, S., Uhlig, C., Luhtanen, A. M., de Jong, J., Janssens, J., Carnat, G., Zhou, J., and Delille, B.: Biogeochemical Impact of Snow Cover and Cyclonic Intrusions on the Winter Weddell Sea Ice Pack, *J. Geophys. Res. Oceans*, 122, 9548–9571, <https://doi.org/10.1002/2017jc013288>, 2017.
- Toyota, T., Takatsuji, S., and Nakayama, M.: Characteristics of sea ice floe size distribution in the seasonal ice zone, *Geophys. Res. Lett.*, 33, <https://doi.org/10.1029/2005gl024556>, 2006.
- 1155 Tsamados, M., Feltham, D., Petty, A., Schroeder, D., and Flocco, D.: Processes controlling surface, bottom and lateral melt of Arctic sea ice in a state of the art sea ice model, *Phil. Trans. A Math. Phys. Eng. Sci.*, 373, <https://doi.org/10.1098/rsta.2014.0167>, 2015.
- Tschudi, M. A., Maslanik, J. A., and Perovich, D. K.: Derivation of melt pond coverage on Arctic sea ice using MODIS observations, *Rem. Sens. Environ.*, 112, 2605–2614, <https://doi.org/10.1016/j.rse.2007.12.009>, 2008.
- 1160 Turner, J. and Comiso, J.: Solve Antarctica's sea-ice puzzle, *Nature*, 547, 275–277, <https://doi.org/10.1038/547275a>, 2017.
- Uotila, P., Vihma, T., Pezza, A. B., Simmonds, I., Keay, K., and Lynch, A. H.: Relationships between Antarctic cyclones and surface conditions as derived from high-resolution numerical weather prediction data, *J. Geophys. Res.*, 116, <https://doi.org/10.1029/2010jd015358>, 2011.
- Urabe, N. and Inoue, M.: Mechanical Properties of Antarctic Sea Ice, *J. Offshore Mech. Arct. Eng.*, 110, 403–
- 1165 408, <https://doi.org/10.1115/1.3257079>, 1988.
- van Loon, H.: The Half-Yearly Oscillations in Middle and High Southern Latitudes and the Coreless Winter, *J. Atmos. Sc.*, 24, 472–486, [https://doi.org/10.1175/1520-0469\(1967\)024<0472:Thyoiim>2.0.Co;2](https://doi.org/10.1175/1520-0469(1967)024<0472:Thyoiim>2.0.Co;2), 1967.
- Vancoppenolle, M., Bopp, L., Madec, G., Dunne, J., Ilyina, T., Halloran, P. R., and Steiner, N.: Future Arctic Ocean primary productivity from CMIP5 simulations: Uncertain outcome, but consistent mechanisms, *Global Biogeochem. Cycles*, 27, 605–
- 1170 619, <https://doi.org/10.1002/gbc.20055>, 2013.
- Vichi, M., Eayrs, C., Alberello, A., Bekker, A., Bennetts, L., Holland, D., de Jong, E., Joubert, W., MacHutchon, K., Messori, G., Mojica, J. F., Onorato, M., Saunders, C., Skatulla, S., and Toffoli, A.: Effects of an Explosive Polar Cyclone Crossing the Antarctic Marginal Ice Zone, *Geophys. Res. Lett.*, 46, 5948–5958, <https://doi.org/10.1029/2019gl082457>, 2019.
- Vihma, T., Johansson, M. M., and Launiainen, J.: Radiative and turbulent surface heat fluxes over sea ice in the western
- 1175 Weddell Sea in early summer, *J. Geophys. Res. Oceans*, 114, <https://doi.org/10.1029/2008jc004995>, 2009.
- Wadhams, P.: The Seasonal Ice Zone. In: *The Geophysics of Sea Ice*, edited by: Untersteiner, N., Springer, Boston, USA, 825–991, https://doi.org/10.1007/978-1-4899-5352-0_15, 1986.
- Wadhams, P.: *Ice In The Ocean*, CRC Press, UK, 364 pp, ISBN 9789056992965, 2000.
- Wadhams, P., Lange, M. A., and Ackley, S. F.: The ice thickness distribution across the Atlantic sector of the Antarctic Ocean
- 1180 in midwinter, *J. Geophys. Res. Oceans*, 92, 14535–14552, <https://doi.org/10.1029/JC092iC13p14535>, 1987.
- Wang, Q., Li, Z., Lu, P., Xu, Y., and Li, Z.: Flexural and compressive strength of the landfast sea ice in the Prydz Bay, East



- Antarctic, The Cryosphere, 16, 1941–1961, <https://doi.org/10.5194/tc-16-1941-2022>, 2022.
- Wang, S., Maltrud, M., Elliott, S., Cameron-Smith, P., and Jonko, A.: Influence of dimethyl sulfide on the carbon cycle and biological production, *Biogeochemistry*, 138, 49–68, <https://doi.org/10.1007/s10533-018-0430-5>, 2018.
- 1185 Warren, S. G.: Optical properties of snow, *Rev. Geophys. Space Phys.*, 20, 67–89, <https://doi.org/10.1029/RG020i001p00067>, 1982.
- Warren, S. G.: Optical properties of ice and snow, *Phil. Trans. A. Math. Phys. Eng. Sc.*, 377, 20180161, <https://doi.org/10.1098/rsta.2018.0161>, 2019.
- Warren, S. G., Hahn, C. J., London, J., Chervin, R. M., and Jenne, R. L.: Global distribution of total cloud cover and cloud
1190 type amounts over the ocean, USDOE Office of Energy Research, Washington, DC (USA). Carbon Dioxide Research Div.; National Center for Atmospheric Research, Boulder (USA), <https://doi.org/10.5065/D6QC01D1>, 1988.
- Webster, M., Gerland, S., Holland, M., Hunke, E., Kwok, R., Lecomte, O., Massom, R., Perovich, D., and Sturm, M.: Snow in the changing sea-ice systems, *Nat. Clim. Ch.*, 8, 946–953, <https://doi.org/10.1038/s41558-018-0286-7>, 2018.
- Webster, M. A., Holland, M., Wright, N. C., Hendricks, S., Hutter, N., Itkin, P., Light, B., Linhardt, F., Perovich, D. K.,
1195 Raphael, I. A., Smith, M. M., von Albedyll, L., and Zhang, J.: Spatiotemporal evolution of melt ponds on Arctic sea ice, *Elem. Sc. Anthropol.*, 10, <https://doi.org/10.1525/elementa.2021.000072>, 2022.
- Weeks, W. F.: *On Sea Ice*, University of Alaska Press, Fairbanks, USA, 664 pp, ISBN 978-1-60223-079-8, 2010.
- Williams, R. G., Ceppi, P., Roussenov, V., Katavouta, A., and Meijers, A. J. S.: The role of the Southern Ocean in the global climate response to carbon emissions, *Phil. Trans. A Math. Phys. Eng. Sc.*, 381, 20220062,
1200 <https://doi.org/10.1098/rsta.2022.0062>, 2023.
- Worby, A. P., Massom, R. A., Allison, I., Lytle, V. I., and Heil, P.: East Antarctic Sea Ice: A Review of Its Structure, Properties and Drift. In: *Antarctic Sea Ice: Physical Processes, Interactions and Variability*, edited by: Jeffries, M. O., Antarctic Research Series, American Geophysical Union, Washington DC, USA, 41–67, <https://doi.org/10.1029/AR074p0041>, 1998.
- Young, I. R. and Ribal, A.: Multiplatform evaluation of global trends in wind speed and wave height, *Science*, 364, 548–552,
1205 <https://doi.org/10.1126/science.aav9527>, 2019.
- Young, I. R., Fontaine, E., Liu, Q., and Babanin, A. V.: The Wave Climate of the Southern Ocean, *J. Phys. Oceanogr.*, 50, 1417–1433, <https://doi.org/10.1175/jpo-d-20-0031.1>, 2020.
- Zatko, M. C. and Warren, S. G.: East Antarctic sea ice in spring: spectral albedo of snow, nilas, frost flowers and slush, and light-absorbing impurities in snow, *Ann. Glaciol.*, 56, 53–64, <https://doi.org/10.3189/2015AoG69A574>, 2015.
- 1210 Zeebe, R. E., Eicken, H., Robinson, D. H., Wolf-Gladrow, D., and Dieckmann, G. S.: Modeling the heating and melting of sea ice through light absorption by microalgae, *J. Geophys. Res. Oceans*, 101, 1163–1181, <https://doi.org/10.1029/95jc02687>, 1996.